Novel amino substituted tetracyclic imidazo[4,5-*b*]pyridine derivatives: Design, synthesis, antiproliferative activity and DNA/RNA binding study

Borka Lončar[a], Nataša Perin[b], Marija Mioč[c], Ida Boček[b], Lea Grgić,[d] Marijeta Kralj[c], Sanja Tomić[d], Marijana Radić Stojković[d*] and Marijana Hranjec[b*]

[a] Pliva d.o.o., odjel TAPI I&R, Unapređenje tehnoloških procesa i Podrška proizvodnji

[b] Department of Organic Chemistry, Faculty of Chemical Engineering and Technology, University of Zagreb, Marulićev trg 19, HR-10000 Zagreb, Croatia

[c] Division of Molecular Medicine, Ruđer Bošković Institute, Bijenička cesta 54, P. O. Box 180, HR-10000 Zagreb, Croatia

[d] Ruđer Bošković Institute, Division of Organic Chemistry and Biochemistry, Bijenička cesta 54, 10 000 Zagreb, Croatia

[*]Corresponding authors: Dr. Marijana Hranjec. Full. Prof., Department of Organic Chemistry, Faculty of Chemical Engineering and Technology, University of Zagreb, Marulićev trg 20, P.O. Box 177, HR-10000 Zagreb, Croatia, Phone No. +38514597245; Fax No. +38514597250; e-mail: mhranjec@fkit.hr; Dr. Marijana Radić Stojković, Ruđer Bošković Institute, Division of Organic Chemistry and Biochemistry, Bijenička cesta 54, 10 000 Zagreb, Croatia; Phone No. 38514571220; e-mail: mradic@irb.hr

Abstract

A novel series of tetracyclic imidazo[4,5-*b*]pyridine derivatives was designed and synthesized as potential antiproliferative agents. Their antiproliferative activity against human cancer cells was influenced by the introduction of chosen amino side chains on the different positions on the tetracyclic skeleton and particularly, by the position of N atom in the pyridine nuclei. Thus, the majority of compounds showed improved activity in comparison to standard drug *etoposide*. Several compounds showed pronounced cytostatic effect in the submicromolar range, especially on HCT116 and MCF-7 cancer cells. The obtained results have confirmed the significant impact of the position of N nitrogen in the pyridine ring on the enhancement of antiproliferative activity, especially for derivatives bearing amino side chains on position 2. Thus, regioisomers **6**, **7** and **9** showed noticeable enhancement of activity in comparison to their counterparts **10**, **11** and **13** with IC_{50} values in a nanomolar range of concentration (0.3 – 0.9 μM). Interactions with DNA (including G-quadruplex structure) and RNA were influenced by the position of amino side chains on the tetracyclic core of imidazo[4,5-*b*]pyridine derivatives and the ligand charge. Moderate to high binding affinities ($\log K_s$ =5-7) obtained for selected imidazo[4,5-*b*]pyridine derivatives suggest that DNA/RNA are potential cell targets.

Key words: amines, imidazo[4,5-*b*]pyridines, antiproliferative activity, DNA/RNA binding

1. Introduction

Due to the structural similarity of imidazo-pyridine heterocyclic system with naturally occurring purines and great therapeutic potential and significance, suchlike derivatives nowadays play an important role in medicinal chemistry and drug discovery.[1] Being one of the chosen privileged building motifs in medicinal chemistry, they showed a wide range of different biological features playing thus an important role in the prevention of numerous diseases. Imidazo-pyridine derivatives foregrounded their importance in the prevention of proper functioning of cancerous cells, diseases related to the central nervous system, inflammation, *etc*. Some of derivatives are known as GABAA receptor positive allosteric modulators,[2] aromatase inhibitors,[3] metalloproteinase inhibitors,[4] DNA/RNA intercalators,[5] proton pump inhibitors,[6] Aurora kinase inhibitors,[7,8] serine/threonine-protein kinase inhibitors [9] or blockers of the gastric proton pump (Fig.1) .[10] Among all possible isomers forms, the most promising biological potential was shown by imidazo[4,5-*b*]pyridine and imidazo[4,5-*c*]pyridine derivatives. The majority of published papers regarding the antitumor activity are describing the inhibition of the different protein kinases caused by mentioned derivatives.

Recently, a group of authors has confirmed the inhibition of Aurora A, B and C kinases, caused by 2-arylimidazo[4,5-*b*]pyridine derivatives and derivatives substituted with 1-benzyl-1*H*-pyrazol-4-yl side chain.[11,12] Additionally, some imidazo[4,5-*b*]pyridines were identified as potent and selective JAK1 and B-Raf kinase inhibitors.[13,14] Furthermore, 2,6-disubstituted imidazo[4,5-*b*]pyridines were identified as highly potent TAM inhibitors.[15] A group of authors has synthesized novel imidazo[4,5-*b*]pyridine derivatives which showed promising anticancer activity against either breast or colon cancer cell lines.[16] Imidazo[4,5-*b*]pyridine derivatives were identified as well as promising c-Met kinase inhibitors with activity against human lung cancer cells.[17] Also, *N*-cyclopentyl substituted 2-aryl/heteroarylimidazo[4,5-*b*]pyridines were shown to be very efficient agents with good microsomal stability.[18]

Since many anticancer drugs base their activity on non-covalent interaction with DNA and RNA, one of our aims was to investigate interactions of prepared ligands with these biological targets. Nucleic acids are due to involvement in many crucial processes in cells (repository and transfer of genetic information, carcinogenesis, gene expression, transcriptional and translational regulation, cell death) molecular targets for a large number of drugs.[21,22]

Hence, the assessment of binding strength and specificity is essential to elucidate the mode of biological action of drugs. The most common and effective non-covalent modes of binding of small molecules to DNA include intercalative and groove binding. Commonly, groove binders are crescent-shaped molecules, consisting of more aromatic rings while intercalators possess planar aromatic surfaces suitable for insertion between DNA bases.[21] However, it is also possible for small molecules (with planar structures and positively charged pendants) to bind to nucleic acids in multiple binding modes (mixed binding mode).

Results of our previously prepared imidazo[4,5-*b*]pyridine derivatives showed that intercalation is a dominant binding mode to DNA. One of these derivatives triggered apoptosis in cancer cells which could be associated with its ability to intercalate into DNA (Fig.1). [5] In a more recent series of substituted benzimidazo[1,2-*a*]quinolines, it was found that one derivative intercalated in the DNA helix and localized in the nucleus. [19] In continuation of this study, some of amino-substituted benzimidazo[1,2-*a*]quinoline DNA intercalators showed weak topoisomerase I poisoning activity. [22] Pyrimidinyl-imidazo[1,2-a]pyridines, dual inhibitors of bacterial DNA gyrase and topoisomerase IV, exhibited antibacterial activity against Gram-positive pathogens, wild-type and methicillin-resistant *Staphylococcus*, and wild-type and fluoroquinolone-resistant *Streptococcus*. [23] A combination of imidazo[1,5-a]pyridine and pyrrolobenzodiazepine scaffolds showed enhanced DNA binding ability (minor groove) and significant antitumor activity. These compounds also induced the expression of proteins involved in apoptosis and DNA damage like p53, p21 and γ-H2AX (Fig.1). [24]

Taking into account a great biological potential and the fact that imidazo[4,5-*b*]pyridine scaffold is among the most privileged and important building blocks in medicinal chemistry, we have designed and synthesized novel tetracyclic derivatives as novel and potent antiproliferative agents. Tetracyclic derivatives were substituted with chosen amino side chains which have significantly enhanced the antiproliferative activity of tetracyclic benzimidazole analogues and are placed at different position of skeleton.[19,20] Additionally, the impact of the N atom position in pyridine nuclei on biological activity was studied.

For chosen counterparts of regioisomers, the DNA (including G-quadruplex structure)/RNA binding affinity was studied by using spectroscopic methods (fluorescence, circular dichroism (CD)) and thermal denaturation experiments. In addition, ligand-DNA/RNA interactions were investigated by molecular docking.

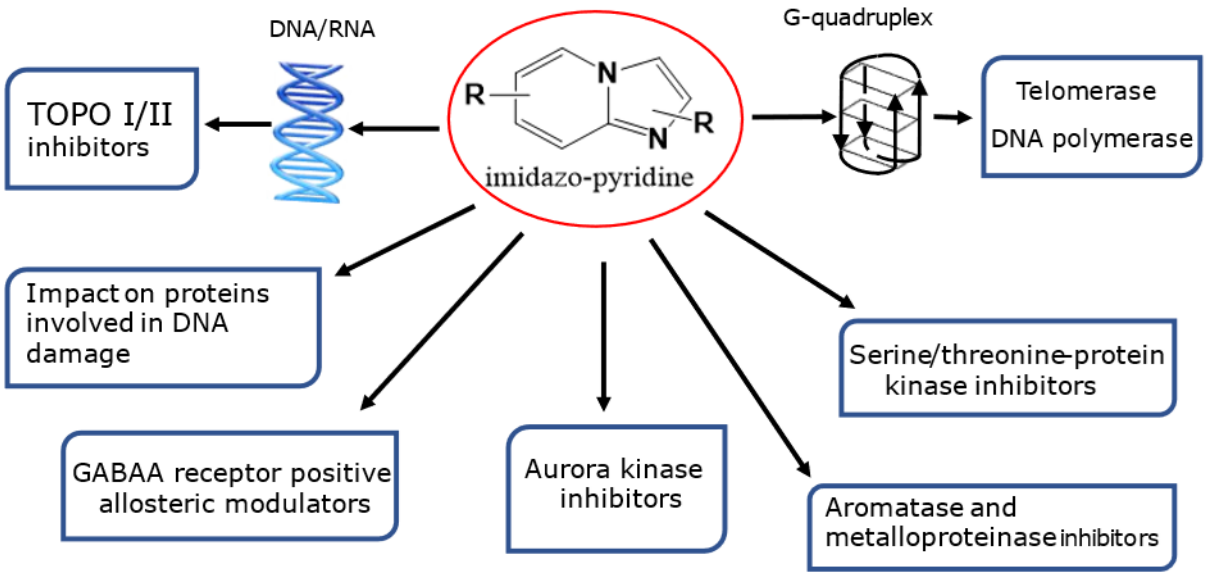

Figure 1. Potential molecular mechanisms of anticancer activity of imidazo-pyridine based compounds

Results and Discussion

1.1. Chemistry

The synthesis of all newly prepared compounds was conducted according to the two main experimental procedures shown in Scheme **1** and **2** using either conventional methods of organic synthesis as well as microwave-assisted synthesis. Acyclic precursors **4**, **16** and **17** were prepared in the reaction of aldol condensation from 2-chloro-4-fluorobenzaldehyde **3** or benzoyl chlorides **14** and **15** with 2-(1*H*-imidazo[4,5-*b*]pyridine-2-yl)acetonitrile **2**. Compound **2** as the main precursor for the synthesis of acyclic derivatives, was obtained in the reaction of cyclocondensation from 2,3-diaminopyridine within the heating with 2-cyanoacetamide at 185 °C. Compound **4** underwent a thermal cyclization in sulfolane to afford cyclic compounds **5a** and **5b** as a mixture of two regioisomers in the ratio 1:1. Regioisomers were successfully separated by column chromatography on SiO_2 using CH_2Cl_2/CH_3OH as eluent. On the other hand, the acyclic compounds **16** and **17** underwent a thermic cyclization in DMF under basic conditions to give the corresponding **18a**/**18b** and **19a**/**19b** as a mixture of regioisomers which at this synthetic point were not separated.

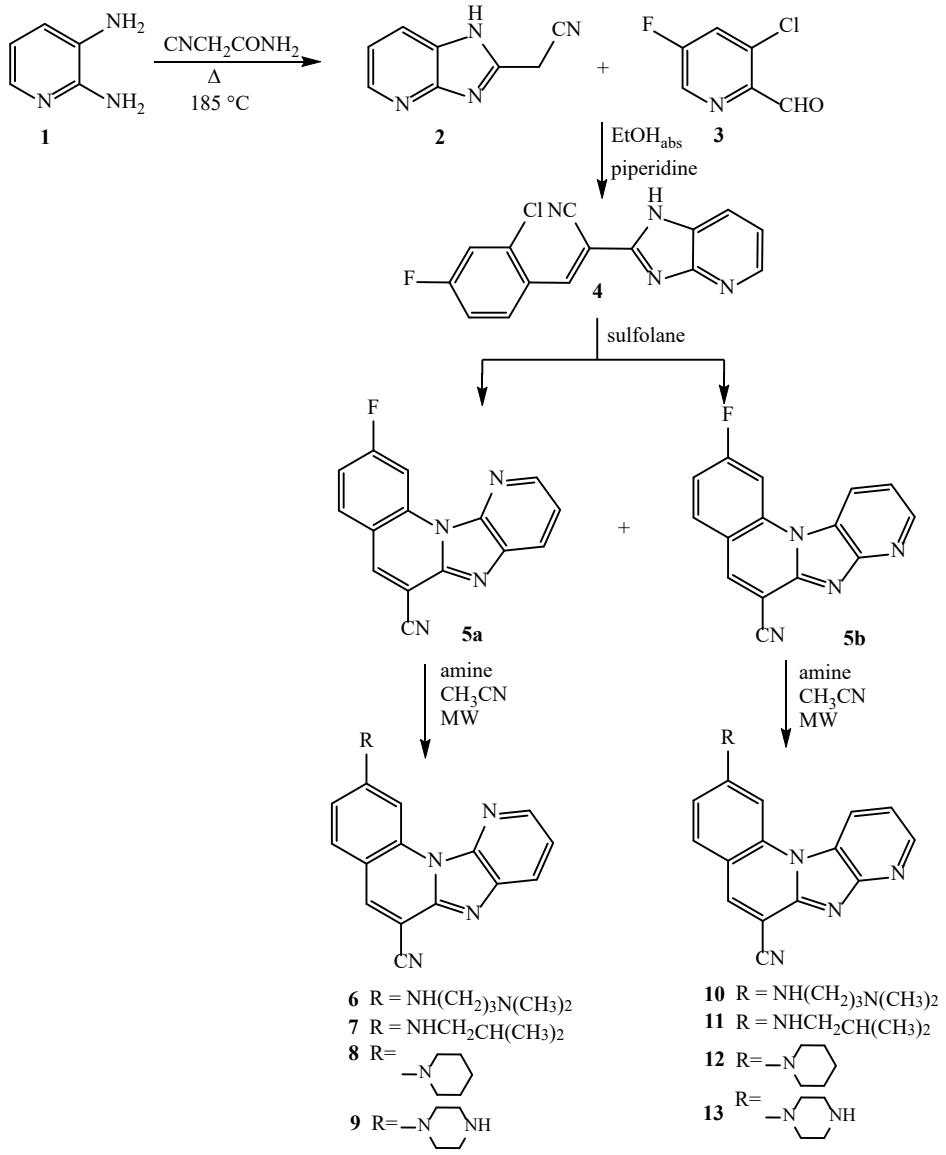

Scheme 1. Synthesis of tetracyclic imidazo[4,5-*b*]pyridine derivatives **6-13**

Subsequent treatment of oxo derivatives with $POCl_3$ and PCl_5 gave the mixture of regioisomers **20:22** (ratio 1:5) and **21:23** (ratio 1:4) which were separated by column chromatography on SiO_2 using CH_2Cl_2/CH_3OH as eluent. Finally, amino (**6–13**) and diamino (**24–37**) substituted pyrido[3',2':4,5]imidazo[1,2-*a*]quinoline-6-carbonitriles and pyrido[2',3':4,5]imidazo[1,2-*a*]quinoline-6-carbonitriles obtained in uncatalyzed microwave-assisted amination from compounds **20–23** by using power 800 W, at 170 °C and 40 bar in acetonitrile with five to seven-fold excess of the appropriate amine. The structures of all prepared compounds were determined by NMR spectroscopy (^1H and ^{13}C) based on the analysis of H-H coupling constants as well as chemical shifts and by elemental analysis.

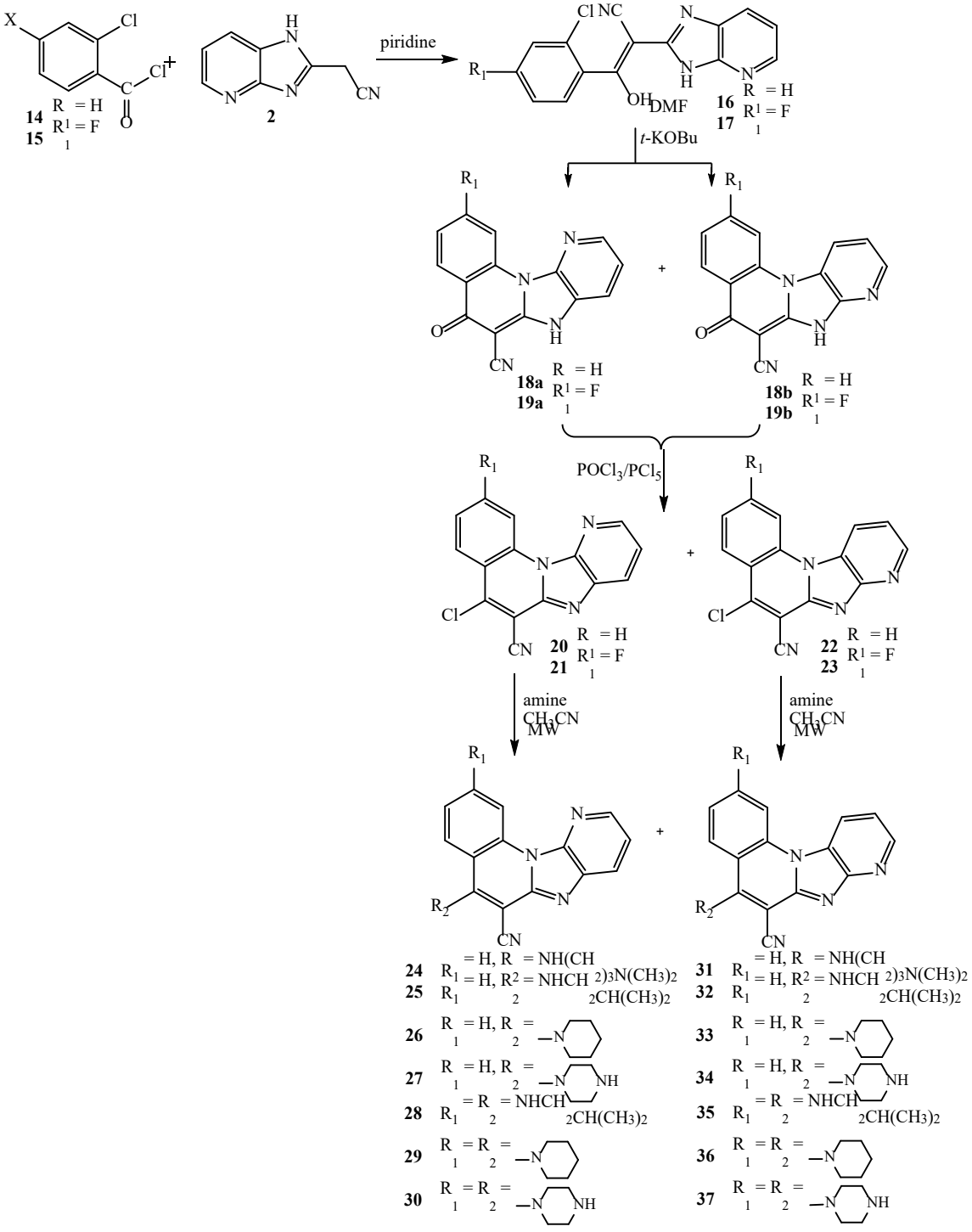

Scheme 2. Synthesis of tetracyclic imidazo[4,5-*b*]pyridine derivatives **24-37**

The structures of regioisomers **24**, **31**, **30** and **37** were additionally confirmed by using 2D NMR spectroscopy. In the NOESY spectra of compounds **31** and **37**, NOE interactions between the H1 and H11 protons of pyridine and benzene nuclei (indicated with green color) confirmed the structure of the regioisomer (Fig. 2).

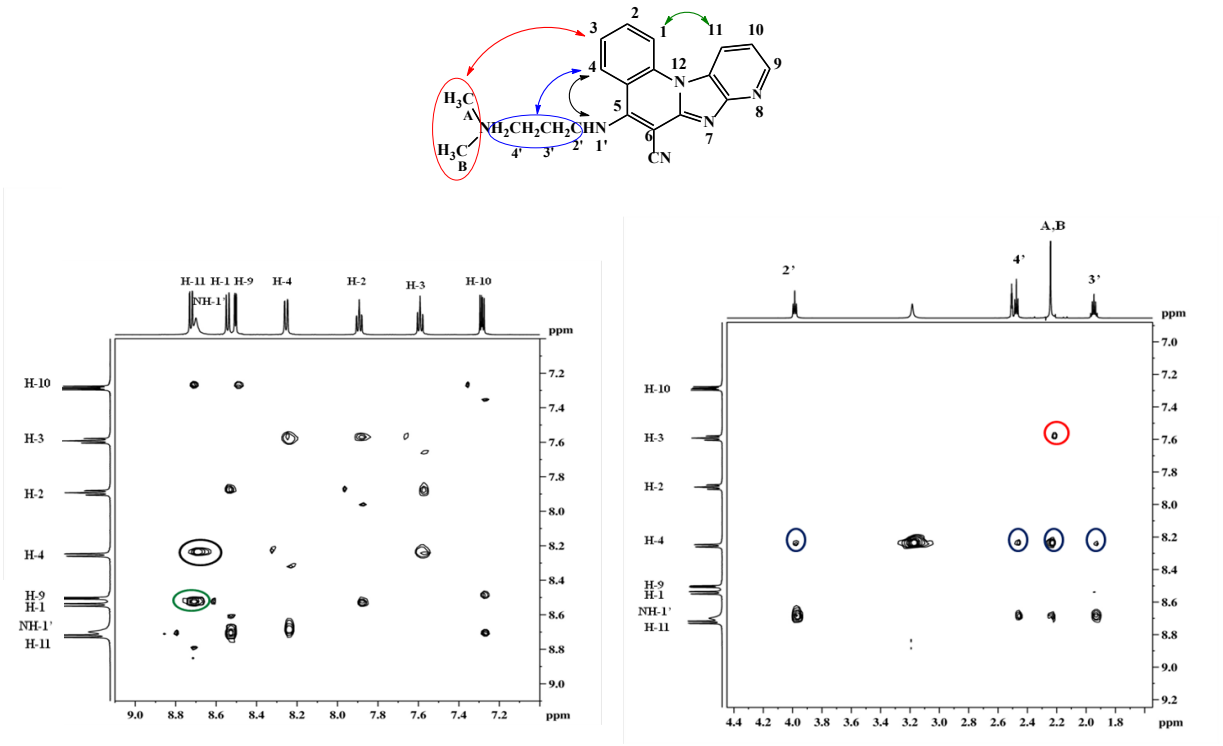

Figure 2. NOESY spectra of 5-*N,N*-dimethylaminopropyl substituted regioisomer **24**

Additionally, the interactions between the protons of the aliphatic part of the molecule, namely the *N,N*-.dimethylaminopropyl side chain with the protons of phenyl ring could be also observed (Fig. 2 and 3).

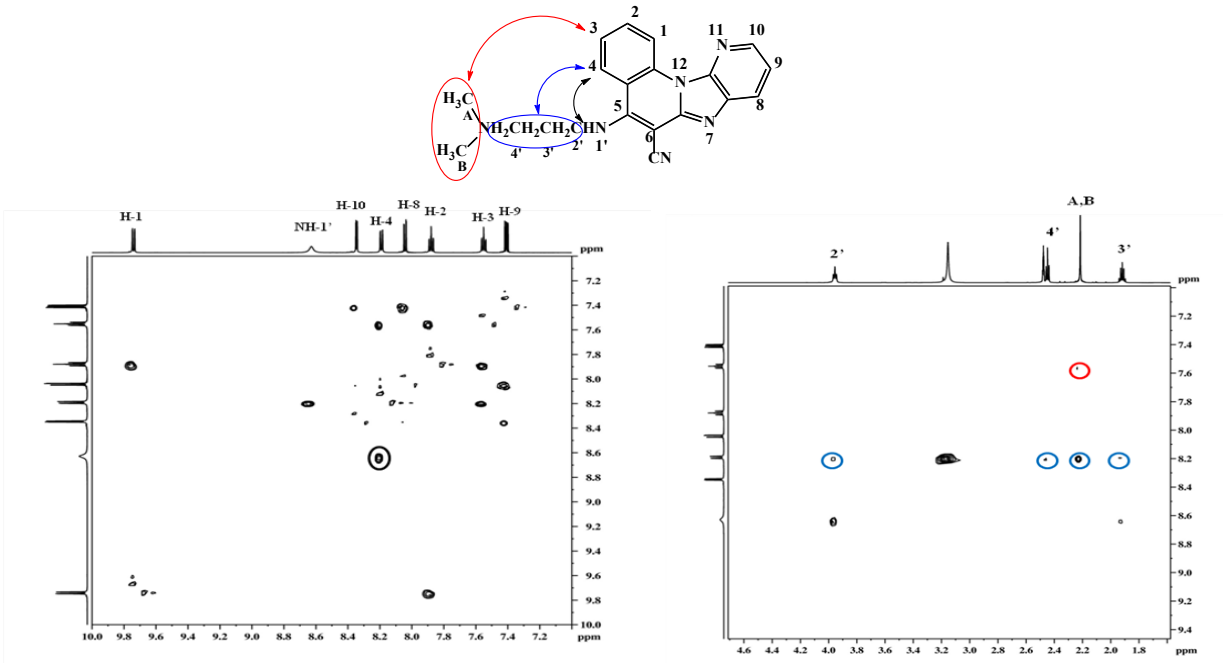

Figure 3. NOESY interactions of 5-*N,N*-dimethylaminopropyl side chain with phenyl ring of regioisomer **24**

1.2. Antiproliferative activity *in vitro*

All newly prepared compounds were first tested against HCT116, MCF-7 and H 460 cancer cell lines to assess their antiproliferative activity *in vitro*. The results are presented in Table 1 and are compared to known antiproliferative agent *etoposide*. In addition, we selected 12 representative derivatives, which either showed the most prominent antiproliferative activities, or evaluated their cytotoxic activity on non-cancerous cells using human embryonic kidney cell line HEK 293. The prepared tetracyclic derivatives were designed with the aim of systematically studying structural effects on antiproliferative features in order to find the positions of amino substituents and N atom in pyridine ring as well as the type of amino substituents which showed the most significant impact on the improvement of the antiproliferative activity.

The obtained results indicated that the majority of tested compounds showed enhanced antiproliferative effect towards cancer cells but without significant selectivity between cancer cells. The exception was fluoro substituted compound **5a**, *N,N*-dimethylaminopropyl substituted derivatives **10**, **24** and **31**, piperazine substituted derivative **13** and chloro substituted derivative **22** with selective activity towards HCT116 cell in comparison to other cancer cells. Several compounds showed improved activity in comparison to standard drug *etoposide*, especially towards HCT116 cells. Interestingly, obtained results revealed that the position of N nitrogen in the pyridine ring had a very strong impact on the enhancement of antiproliferative activity. Regioisomers **6**, **7** and **9** bearing amino substituents on the position 2 of tetracyclic skeleton, showed significant improvement of activity in comparison to their counterparts **10**, **11** and **13** having IC_{50} values in a nanomolar range of concentration (0.3 – 0.9 μM). Regarding the 5-amino substituted regioisomers, it could be observed that the position of N atom did not significantly influence the antiproliferative activity. Furthermore, only 2,5-dipiperazinyl substituted regioisomer **30** showed better activity compared to its regioisomer **37** which surprisingly did not show any inhibitory effect at all. The type of amino side chains was chosen based on previously published results for benzimidazole-derived tetracyclic derivatives. As it could be observed, there was no significant difference in the influence of *N,N*-dimethylaminopropyl, *N*-isobutyl and piperazine side chain on antiproliferative activity with the exception of mono-piperidine substituted derivatives **8** and **12** which showed the lowest antiproliferative effect.

Table 1. Antiproliferative activity of tested compounds and their clogP values

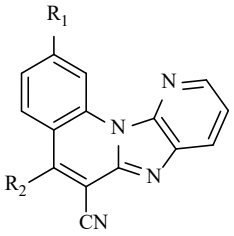

5a, 6-9, 20-21, 24-30

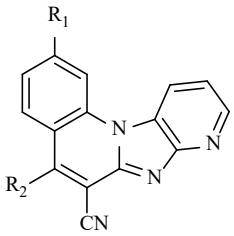

5b, 10-13, 22-23, 31-37

Compd	R_1	R_2	IC_{50}[a] (μM)				clogP[b]
			HCT116	*MCF-7*	*H460*	*HEK 293*	
5a	F	H	5±1.4	≥100	≥100	n.t.[c]	2.86
5b	F	H	≥100	≥100	≥100	n.t.	2.86
6	$NH(CH_2)_3N(CH_3)_2$	H	0.4±0.08	0.7±0.1	0.4±0.1	0.3±0.08	3.34
7	$NHCH_2CH(CH_3)_2$	H	0.5±0.02	0.4	0.3±0.05	0.5±0.2	4.26
8	piperidine	H	5.5±1.5	3±0.9	≥100	n.t.	3.87
9	piperazine	H	0.4±0.06	0.4±0.1	0.4±0.08	0.7±0.4	2.47
10	$NH(CH_2)_3N(CH_3)_2$	H	2.3±0.5	12±4.5	11±1.7	4±0.09	3.34
11	$NHCH_2CH(CH_3)_2$	H	3±1.7	3±2	12±4	n.t.	4.26
12	piperidine	H	10±2.7	5±4.5	49±0.01	n.t.	3.87
13	piperazine	H	0.9±0.8	3.1±1.2	7±0.7	n.t.	2.47
20	H	Cl	3±3	6±4	≥100	n.t.	3.30
21	F	Cl	3±0.06	2 ±0.6	≥100	n.t.	3.44
22	H	Cl	0.1±2	2±0.4	4.6±1.6	1.6±0.1	3.30
23	F	Cl	3.5±2	2±0.8	≥100	n.t.	3.44
24	H	$NH(CH_2)_3N(CH_3)_2$	0.9±0.03	2.9±1.3	1.4±0.2	1.8±0.2	3.72
25	H	$NHCH_2CH(CH_3)_2$	≥100	≥100	≥100	>100	4.64
26	H	piperidine	47±0.6	16±1.3	≥100	n.t.	4.08
27	H	piperazine	3.6±0.3	4.7±0.5	1.8±1	n.t.	2.68
28	$NHCH_2CH(CH_3)_2$	$NHCH_2CH(CH_3)_2$	3±0.2	1.8±0.3	5.4±0.4	n.t.	5.78
29	piperidine	piperidine	1±0.8	0.5±0.2	≥100	>100	5.04
30	piperazine	piperazine	0.4±0.05	0.4±0.0	0.7±0.4	0.2±0.1	2.25
31	H	$NH(CH_2)_3N(CH_3)_2$	0.8±0.1	3.2±0.5	2±0.1	2.6±0.7	3.72
32	H	$NHCH_2CH(CH_3)_2$	14±2.7	14±3.5	17.5±0.7	>100	4.64
33	H	piperidine	≥100	≥100	≥100	n.t.	4.08
34	H	piperazine	3.5±1.2	3±2.8	7±0.6	n.t.	2.68
35	$NHCH_2CH(CH_3)_2$	$NHCH_2CH(CH_3)_2$	3.7±0.4	2 ±0.7	7.6±0.5	n.t.	5.78
36	piperidine	piperidine	1.8±0.1	3.6±0.6	7±3.5	n.t.	5.04
37	piperazine	piperazine	≥100	≥100	≥100	>100	2.25
Etoposide	-	-	5±2	1±0.7	0.1±0.04	-	-

[a] IC_{50}; the concentration that causes 50% growth inhibition; [b] clogP; calculated logP values were obtained by using ChemDraw Professional 15.0.; c) not tested.

Additionally, we have also tested halogen substituted derivatives with compound **22** bearing chloro group at position 5 being the most active one ($IC_{50(HCT116)}$ 0.1 μM). The results obtained from the testing against non-tumour cells showed that 12 tested compounds had a relatively similar cytotoxic profile in tumour cells in comparison to non-tumour cells with the exception of *N*-isobutyl substituted derivative **32** which showed to be non-cytotoxic (IC_{50} > 100 μM). Interestingly, compound **22** showed significantly lower activity (~16 times) against HCT116 cells in comparison to non-tumour cells.

Considering the lipophilicity of imidazo[4,5-*b*]pyridine derivatives, the clogP values increased upon the introduction of *N*-isobutyl side chain at all positions on the tetracyclic skeleton. A significant decrease in lipophilicity was observed upon the introduction of the piperazine ring. Piperidine substituent caused slight decrease of clogP value in comparison to *N*-butyl side chain and an increase compared to compounds bearing *N,N*-dimethylaminopropyl side chain.

1.3. DNA/RNA binding study

1.3.1. Interactions with double-stranded (ds-) polynucleotides

Based on the results of antiproliferative activity, we have chosen six compounds for study with nucleic acids. Compounds **10, 6, 37, 30, 32** and **25** were soluble in water (c=3 × 10^{-3} mol dm^{-3}). The absorbancies of buffered aqueous solutions of studied compounds were proportional to their concentrations up to c=3 × 10^{-5} mol dm^{-3}. Such behavior suggests that studied compounds do not aggregate by intermolecular stacking at experimental conditions used. Absorption maxima and corresponding molar extinction coefficients (ε) were given in Fig. 4 and Table S1 (Supporting information, SI).

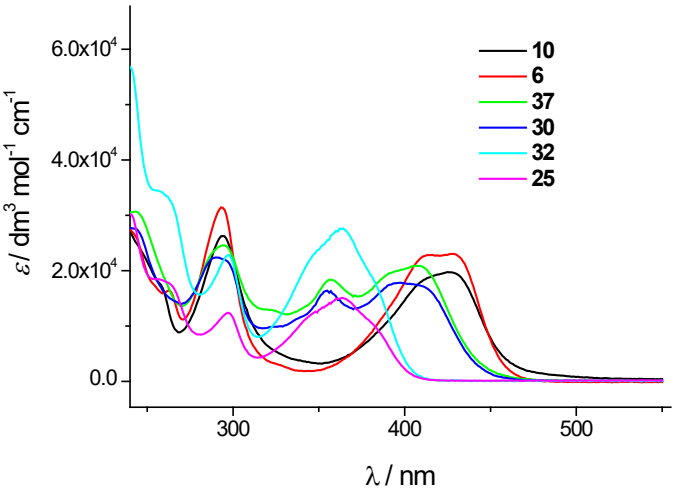

Figure 4. UV/Vis spectra of **10, 6, 37, 30, 32** and **25** at c ≈ 1× 10^{-5} mol dm^{-3} ; pH=7, sodium cacodylate/HCl buffer, I = 0,05 mol dm^{-3}.

Fluorimetric measurements were performed in an area where the emission and excitation spectra do not overlap. Chemicalize software was used for the prediction of pKa values of imidazo[4,5-*b*]pyridine derivatives (or simply **IP** derivatives). At pH 7.0 **10** and **6** possess one positive charge, piperazine derivatives (**37**, **30**) two charges while isobutylamino derivatives **25** and **32** were not charged.[25]

The binding study with DNA and RNA was carried out with ctDNA, AT-DNA (poly(dAdT)$_2$) and GC-DNA (poly(dGdC)$_2$), as models for classical B-helix and AU-RNA (poly A – poly U), as a model for A-helix.[26] Titration with GC-DNA yielded fluorescence decrease/quenching of all studied compounds. Addition of AU-RNA and AT-DNA to buffer aqueous solution of **37**, **30**, **32** and **25** resulted in an emission increase of those compounds (Table 2, Fig. 5, SI). In contrast to that, **10** and **6** emission decreased in titrations with AU and AT polynucleotides. The position of amino side chains on the tetracyclic ring most likely influenced the fluorescence changes since, in the case of **10** and **6**, the addition of AT- and AU-sequences did not cause an increase in their emission (Table 2, SI). The position and the nature of the substituent on a heterocyclic ring have a significant impact on the electron density of aromatic systems which in turn may influence its binding orientation and fluorescence properties upon interaction with nucleic acids.[27-29] In this case, C-2 (in **10** and **6**) and C-5 (in **37**, **30**, **32** and **25)** amino side pendants cause redistribution in electron densities of the aromatic core which results in either a decrease in fluorescence (**10** and **6** with all polynucleotides and **37**, **30**, **32** and **25** with GC sequences) or its increase (**37**, **30**, **32** and

25 with AT/AU sequences). Also, it can be noticed that the addition of ctDNA caused a decrease in fluorescence of the majority of compounds which can be probably ascribed to the mixed basepair composition of this natural polynucleotide (about 42% GC base pairs). Similar opposite fluorescence responses with AT and GC sequences, noticed with **37**, **30**, **32** and **25**, were previously observed in few compounds (acridine and phenanthridine derivatives, 4,9-diazapyrenium cations).[30-32] Such changes have been associated with intercalation of the abovementioned hetero/polycyclic compounds to ds-DNA/RNA since only π-π stacking interactions with the most electron-donating nucleobase, guanine result in efficient fluorescence quenching.[33]

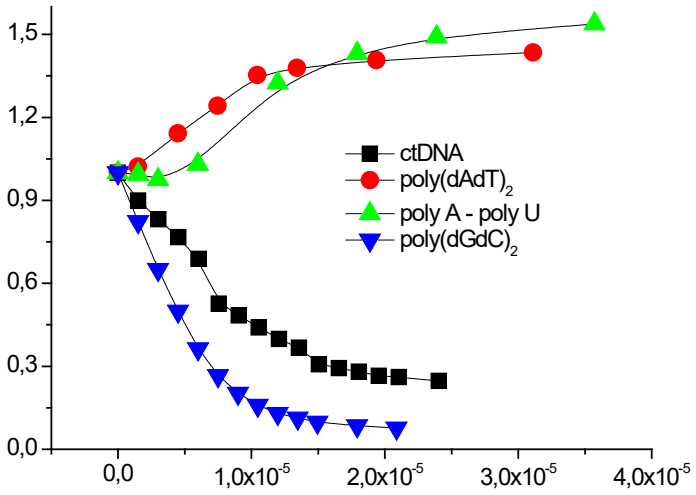

Figure 5. Fluorescence changes of **30** (c= 1.5-2 × 10^{-6} mol dm^{-3}; λ_{ex}=397 nm) upon titration with ctDNA (■), poly(dAdT)$_2$(●), poly A-poly U (▲), poly(dGdC)$_2$ (▼).

The binding constants *Ks* and ratios $n_{[\text{bound compound}]/\,[\text{DNA/RNA}]}$ were calculated by the processing of fluorimetric titration data with the Scatchard equation[35] (Table 2). Fluorescence changes of **25** with some polynucleotides were too small or linear for the accurate calculation of binding constants. While fluorescence changes depended mostly on the position of amino side chains on the tetracyclic ring, the strength of the interactions with DNA/RNA was influenced by both, the position of the amino side chain and the ligand charge.

Table 2. Binding constants (log*Ks*)[a] and ratios *n*[b] ([bound compound]/ [polynucleotide phosphate]) calculated from the fluorescence titrations of **10, 6, 37, 30, 32** and **25** with ds-polynucleotides at pH = 7,0 (buffer sodium cacodylate, I = 0,05 mol dm^{-3}).

Cpd	ctDNA			poly A - poly U			p(dAdT)$_2$			p(dGdC)$_2$		
	logK_s	*n*	I/I$_0$[c]	logK_s	*n*	I/I$_0$[c]	logK_s	*n*	I/I$_0$[c]	logK_s	*n*	I/I$_0$[c]
10	6.0	0.4	0.5	5.5	0.4	0.8	6.4	0.4	0.8	5.6	0.4	0.4
6	5.5	0.6	0.5	6.3	0.1	0.8	6.9	0.2	0.7	5.8	0.2	0.4
37	6.4	0.1	0	6.5	0.1	1.8	6.8	< 0.1	1.3	6.6	0.2	0
30	6.3	0.3	0.1	6.6	0.1	2.0	6.8	0.2	1.5	6.8	0.3	< 0.1
32	4. 5	< 0.1	2.2	4.7	0.1	7.1	5.1	< 0.1	8.3	5.5	< 0.1	0.5
25	-[d]	-[d]	-[d]	5.3	< 0.1	2.5	4.6	0.1	10.4	-[d]	-[d]	-[d]

[a] Accuracy of n ± 10 - 30%, consequently log*Ks* values vary in the same order of magnitude;
[b] Processing of titration data using Scatchard equation[34,35] gave values of ratio *n*[bound compound]/[polynucleotide] except in titrations of **30** with poly(dAdT)$_2$ and **32** with poly A ‑ poly U where the ratio *n* had to be fixed to a certain value (SI).
[c] I_0 – starting fluorescence intensity of **10**, **6**, **37**, **30**, **32** and **25**; I – fluorescence intensity of **10**, **6**, **37**, **30**, **32** and **25**/ polynucleotide complex calculated by Scatchard equation.
[d] small or linear fluorescence change disabled calculation of stability constant.

Thus **10** and **6** with amino side pendant (dimethylaminopropylamino) at C-2 position with one positive charge and **37** and **30** with piperazine at C-2 and C-5 positions with two positive charges showed greater affinities towards ds-DNA and ds-RNA compared to **32** and **25** with isobutylamino at C-5 position possessing no net positive charges (Table 2).

Thermal melting (T_m) value is an important factor in the characterization of compound/polynucleotide interactions. ΔT_m value is a difference between the T_m value of free polynucleotide and complex with a small molecule.[36] In general, the intercalative way of binding stabilizes ds-nucleic acids and yields positive ΔT_m values while minor groove binders may cause stabilization (positive ΔT_m values) or destabilization of ds-DNA/RNA (negative ΔT_m values). **10**, **6**, **37** and **30** showed moderate to big stabilization effects of ctDNA and AT/AU polynucleotides (Table 3, Fig. 6, SI).

32 and **25** showed a small or no stabilization effect of polynucleotides. Like with binding affinities, such negligible stabilization effect of **32** and **20** can be related to different positions of the amino side chains on the tetracyclic skeleton and the ligand charge.

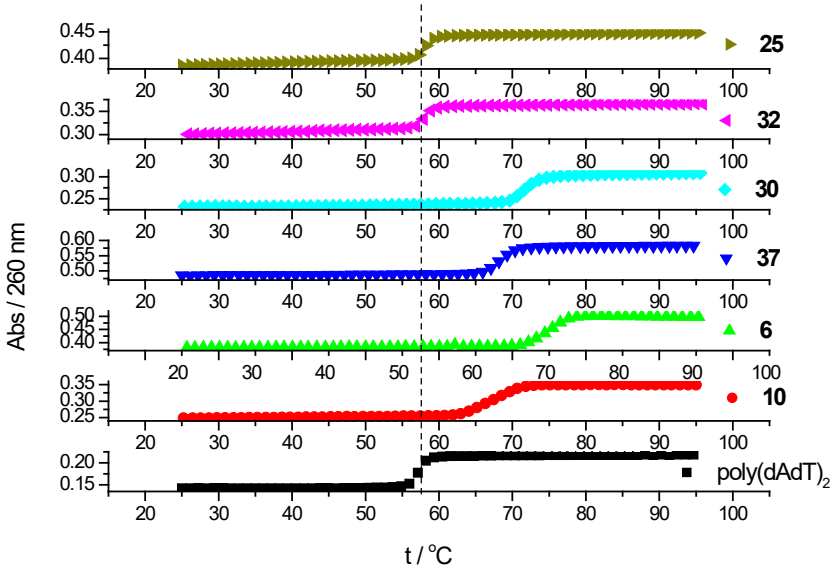

Figure 6. a) Melting curve of **poly(dAdT)$_2$** upon addition of ratio, ***r*** ([compound/ [polynucleotide])=0.3 of **10, 6, 37, 30, 32** and **25** at pH = 7.0 (buffer sodium cacodylate, I = 0.05 mol dm^{-3}).

Table 3. The [a]ΔT_m values (°C) of studied ds- polynucleotides upon addition of ratio [b]***r*** =0.3 of **10, 6, 37, 30, 32** and **25** at pH 7.0 (sodium cacodylate buffer, I = 0.05 mol dm^{-3}).

[b]***r*** = 0.3	10	6	37	30	32	25
ctDNA	4.2	6.6	6.6	7.5	0	0.8
poly A - poly U	[c]4.5/16.5	[c]9.5/23.5	[c]13.5/27.5	[c]15/27	0.6	0
poly(dA- dT)$_2$	9.9	18.2	11.1	14.3	0	0.8

[a] Error in ΔT_m : ± 0.5°C;
[b] ***r*** = [compound] / [polynucleotide]
[c] Biphasic thermal denaturation transitions

Higher ΔT_m values displayed by **10**, **6**, **37** and **30** towards AT/AU polynucleotides in comparison to ctDNA can be attributed to the mixed basepair composition of ctDNA. Also, it was noted that regioisomer **6** showed higher values of ΔT_m for AT-DNA and AU-RNA than the other regioisomer **10** (Table 3, SI).

To obtain information on the conformation of nucleic acids and its change due to interaction with small molecules, we used CD spectroscopy. CD spectroscopy can also provide insight into the modes of interactions based on the mutual orientation of the small molecule and the nucleic acid chiral axis.[37]

Achiral small molecules such as **IP** derivatives may also produce induced CD spectrum (ICD) after binding to nucleic acids. Since these compounds possess UV/Vis spectra in the region from 240 to 500 nm, the observed ICD spectra at the wavelengths > 300 nm, where nucleic acids do not absorb, can be attributed to them (Fig. 7, SI).

Generally, the addition of **10**, **6**, **37** and **30** caused greater changes (increase/decrease) in CD spectra of DNA/RNA polynucleotides compared to **32** and **25** (Fig. 7, SI). Besides, significant ICD bands appeared in titrations of **10**, **6**, **37** and **30** with studied polynucleotides. With AT-DNA, **10** and **6** caused the increase in the intensity of CD signal around 273 nm (where both ligands and DNA absorb) and positive ICD signals positioned at 305 nm. Also, **6** induced the appearance of bisignate signals in the area from 370 – 490 nm while **10** induced negative ICD signals positioned around 445 nm. These changes could be the consequence of mixed binding mode - minor groove binding and binding of aggregated **10** and **6** molecules along the polynucleotide backbone and possibly inside the hydrophobic major groove.[38]

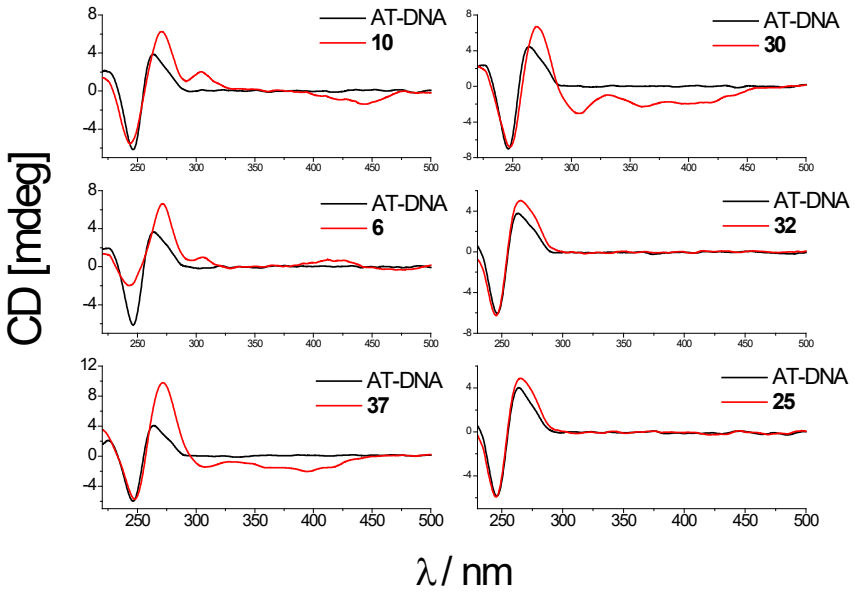

Figure 7. CD titration of AT-DNA (poly dAdT)$_2$, c = 3.0 × 10^{-5} mol dm^{-3}) with **10, 6, 37, 30, 32** and **25** at molar ratios **r** = 0.5 (pH = 7.0, buffer sodium cacodylate, I = 0.05 mol dm^{-3}).

ICD signals like those induced with AT-DNA but smaller in intensity (probably due to guanine amino group protruding into the minor groove and hindering the interaction) were noticed in CD spectra of GC-DNA upon addition of **10** and **6**.

The addition of **10** and **6** to poly A-poly U solution caused a small decrease in intensity of CD spectra of RNA and the formation of weak negative ICD signals around 305 nm (SI). Such changes in ICD signals usually imply an intercalative binding where the ligand with its longer axis is positioned parallel to the longer axis of the adjacent base pair.[38] Rather similar changes in ICD spectra were observed in CD titrations of **37** and **30** with all studied ds-polynucleotides. In most titrations, a weak negative ICD signal was formed at ratio $r \leq 0.1$ and stronger negative signals from 300 to 450 nm were noticed at ratios higher than $r > 0.1$. Changes at lower ratios could be associated with the intercalation while at higher ratios they were most probably the result of binding of aggregated molecules along the polynucleotide backbone (Fig. 7, SI). Most likely, this type of binding is dominant at higher ratios due to the bulkiness of piperazine groups that hampers the insertion of the tetracyclic core between nucleobases.

However, since these compounds induced different fluorescence responses, increase with AT-DNA and quenching with GC base pairs, it is possible that at lower ratios they partially intercalate only in GC-rich DNA. **32** and **25** induced observable changes (slight increase) only in CD spectra of AT-DNA (Fig. 7, SI). The addition of **25** in ctDNA solution caused an appearance of small negative CD signals around 305 nm which may suggest an intercalative mode of binding. Nevertheless, since these compounds do not stabilize ds-DNA/RNA, an intercalative binding mode can be excluded. A small decrease in the intensity of CD spectra of GC-DNA could be a result of partial intercalation or groove binding where the long axes of the tetracyclic ring and adjacent base pairs are positioned at an angle to each other resulting in the abolition of positive and negative contributions (SI).[39] These negligible changes observed in most CD titrations of **32** and **25** agree well with the calculated binding affinities and absence of thermal stabilization of DNA and RNA.

Some of the suggested ways of binding were also examined by molecular docking. Interactions of **6** and **32** with alternating double-stranded copolymer, poly(dA-dT)·poly(dA-dT) are shown in the Figure 8. Modes of binding for **6** and **32** with AT-DNA suggested by the spectroscopic methods were consistent with the results obtained by molecular docking.

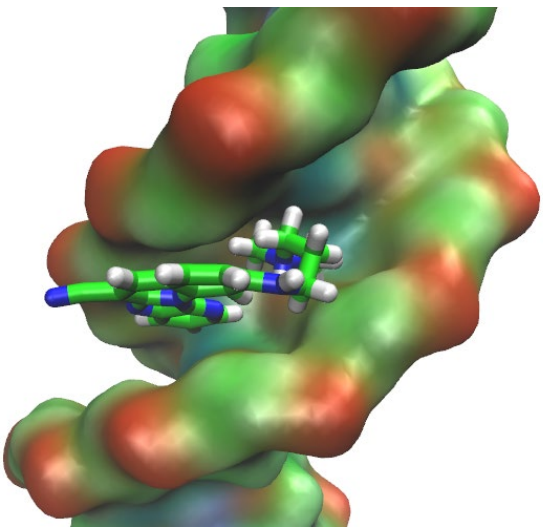

a)

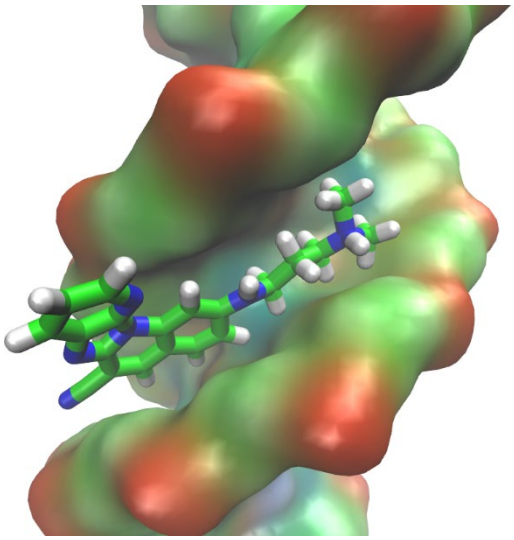

b)

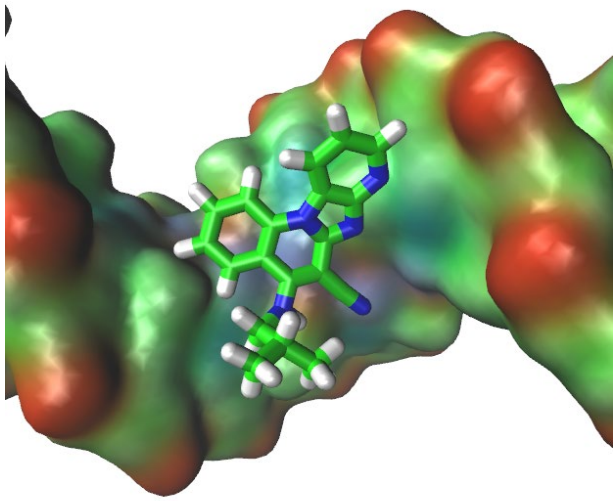

c)

Figure 8. a) and b) DNA-**6** complexes obtained after 10 and 20 ns of MD simulation in water, respectively, starting from two different initial orientations of **6** in DNA. c) DNA-**32** complex obtained after 1 ns of MD simulation in water. (Complexes were built using the PyMOL program wherein the initial position of ligands was determined from spectroscopic data. Parametrization was performed by ANTECHAMBER [40] and Leap, the modules available within AMBER16 suit of programs [41,42] using GAFF [43] for the ligands and OL15 for DNA. Neutralized and solvated complexes were minimized, equilibrated and simulated for 20 ns using programs sander and pmemd.).

According to the binding free energies, calculated by the program MMPBSA.py [44], for orientations of **6,** shown in Fig. 8 a) and b) are -43 ± 4 kcal/mol and -46 ± 3 kcal/mol, respectively. Apparently, both orientations are similarly stable.

2.3.2. Interactions with G-quadruplex

We have also investigated the binding of ligands with G-quadruplex DNA quadruplex, a target thought to be associated with significant biological processes, among else cancer growth and progression.[45] **IP** derivatives possess structural characteristics (flat aromatic surfaces, positively charged side chains with the exception of **25** and **32**) that could allow good recognition of G-quadruplex and potentially selectivity for quadruplex over duplex DNA. As a model for the human telomere sequence, we have used 22 nt sequence (d[AGGG(TTAGGG)$_3$], Tel 22). Depending on the applied methodology (NMR, X-ray crystallography, biophysical studies) and the variants of the human telomere sequence, different hybrid forms exist in K^+ environment.[45-47] Xu and others implied that 22 nt telomere sequence in K^+ solution exists as a mixture of mixed-parallel/antiparallel and chair-type G-quadruplex.[48] Titration with Tel22 yielded fluorescence decrease of the majority of studied compounds (**10**, **6**, **37** and **30**), except with **32** and **25** whose emission increased (Table 4, Fig. 9, SI). Interestingly, the emission of **32** and **25** decreased upon interaction with ds-GC polynucleotide. The obtained result could indicate the importance of the length of π-stacked DNA systems where quenching of emission of the fluorophore with guanine can be accomplished only within longer DNA molecules.[33]

The data from fluorimetric measurements were used for the calculation of the binding constants (log K_s) and stoichiometries of complexes in the concentration range that correspond to 20-80% complex formed (Table 4, Fig. 9). The experimental data of **37** and **30** were best fitted to a binding stoichiometry of ligand-Tel22 of 1:1 and 1:2. In addition, the highest constants were obtained for 1:2 **37**/**30**-Tel22 complexes. 1:1 stoichiometries were found for complexes of Tel22 and **10**, **6**, **32** and **25** with rather similar log Ks values (Table 4). The smallest log Ks values to Tel22 showed **32** and **25** possessing isobutylamino side pendant at C-5 position and no charges. Studied ligands exhibited a moderate stabilization effect of Tel22. The greatest stabilization effect was shown by **37** with piperazine groups at C-2 and C-5 positions (Table 4).

Table 4. Binding constants (log*Ks*)[a] for 1:1 and 1:1/1:2 complexes of **IP**-Tel22 and changes of fluorescence intensity I/I_0[b] calculated from the fluorescence titrations and ΔT_m[d] values (°C) of Tel22 upon addition of ratio[e] ***r*** = 1 of **IP** derivatives at pH = 7.0 (potassium phosphate buffer, I = 0.1 mol dm^{-3}).

compound	logK_s	I/I_0[b]	ΔT_m / °C
10	5.35±0.03	0.66	2.0
6	5.48±0.03	0.70	1.9
37	7.16±0.2 5.33±0.2	0.89 0.62	2.5
30	6.85±0.09 5.04±0.45	0.81 0.77	-[c]
32	4.69±0.02	4.75	1.4
25	4.51±0.05	5.52	1.8

[a] Stability constant Ks and stoichiometry calculated by processing the titration data using non-linear least-square SPECFIT program[49]

[b] Changes in fluorescence of BXLs induced by complex formation (I_0 was emission intensity of free compound and I_{lim} was emission intensity of a complex, calculated by processing the titration data using SPECFIT program).

[c] Changes of **30** with the temperature rise at a concentration equivalent to ratio 1 were too great so it was not possible to determine the ΔT_m value;

[d] Error in ΔT_m: ± 0.5 °C;

[e] ***r*** = [compound]/[polynucleotide].

A positive band at 290 nm and a shoulder at 260 nm, characteristic of mixed-parallel/antiparallel arrangement, were visible in CD spectrum of Tel 22 in K^+ solution (SI).[49-51] Intensities of the CD band of Tel 22 were not greatly modified upon the addition of studied ligands. All compounds caused a small increase of CD band of Tel22 at 290 nm (SI) and a small to moderate (especially **10** and **6**) decrease of the shoulder at 250 nm. Similar changes obtained in CD titrations of Tel22 with all compounds suggest a similar way of binding (for 1:1 complexes), most probably stacking on one of the terminal quartets of Tel22.[52]

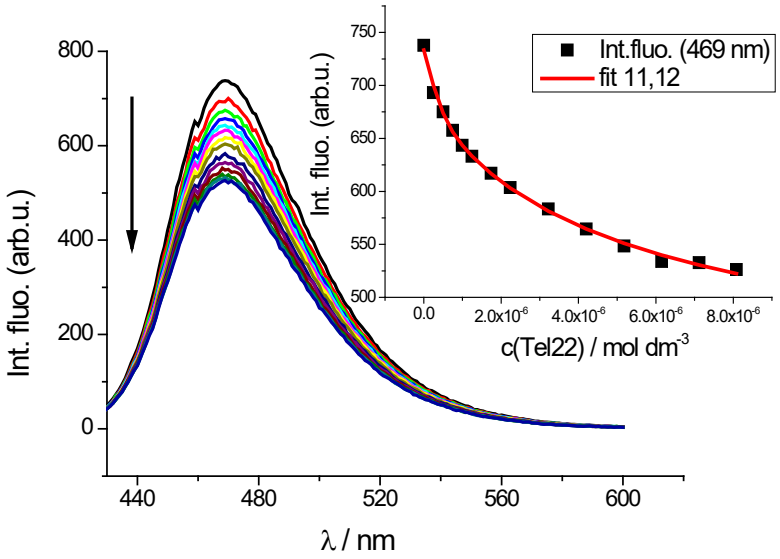

Figure 9. Changes in fluorescence spectrum of **37** (c= 5,0 × 10^{-7} mol dm^{-3}, λ_{exc}=408 nm) upon titration with Tel22 (c= 2,5 × 10^{-7} – 8,1 × 10^{-6} mol dm^{-3}); Inset: Experimental (■) and calculated (—) fluorescence intensities of **37** at λ_{em} = 469 nm upon addition of Tel22 (pH = 7.0, K phosphate buffer, I = 0.1 mol dm^{-3}).

On the other hand, **37** and **30** in 1:2 complexes with Tel22 most probably bind between terminal quartets at the interface of the two quadruplexes. However, to determine an accurate and preferred topology for Tel22-ligand complex,[53] additional experiments (NMR, x-ray crystal structure, molecular modeling) should be performed, that goes beyond the scope of this paper. Although the selectivity for quadruplex over duplex DNA was not achieved, due to the good recognition potential of Tel 22, **37** and **30** structures could be further optimized through additional functionalization of piperazine side chains at C-2 and C-5 positions.

2. Conclusions

Within this work, we have described the design and synthesis of tetracyclic systems based on the imidazo[4,5-*b*]pyridine nuclei which were substituted with amino substituents chosen according to the previously published results for benzimidazole analogues. The antiproliferative activity of regioisomers was studied against human cancer cells and non-tumour cells in order to get insight into the impact of the different position and type of amino side chains and particularly, and the influence of the N atom position in pyridine nuclei.

The majority of compounds showed improvement of antiproliferative activity on HCT116 and MCF-7 cancer cells when compared to a standard drug *etoposide*. From the obtained results it could be noticed that the position of N nitrogen in the pyridine ring has a strong impact on the antiproliferative activity, while the type of amino substituent did not influence activity significantly. Thus, regioisomers **6**, **7** and **9** substituted with amino substituents at position 2 showed noticeable enhancement of activity in comparison to their counterparts **10**, **11** and **13** having IC_{50} values from 0.3 μM to 0.9 μM against all three cancer cells.

Furthermore, chosen compounds had a relatively similar cytotoxic profile in tumour cells in comparison to non-tumour cells. The exception was compound **32** substituted with *N*-isobutylamino group being non-cytotoxic (IC_{50} > 100 μM).

DNA (including G-quadruplex structure)/RNA binding strength was affected by the position of the amino side chain on the tetracyclic core of imidazo[4,5-*b*]pyridine derivatives and the ligand charge. At lower compound to polynucleotide ratios (many data points at $r \leq 0.1$ in fluorescence titrations and data at $r \leq 0.1$ in CD titrations, Table 2 and Fig. 7), obtained results (1-10 μM, positive ICD signals in the region from 273-305 nm noticed for AT- and GC-DNA and weak negative ICD signals around 305 nm for AU-RNA, enhanced thermal stability of polynucleotides) suggest that **10** and **6** bind inside the minor groove of AT- and GC-DNA and intercalate into AU-RNA. Derivatives **37** and **30** with piperazine most probably bind by intercalative binding mode (negative ICD signals, moderate to big ΔT_m values) while lower affinities of **32** and **25** in comparison to **10**, **6**, **37** and **30**, and absence of thermal stability, as well as negligible ICD signals, point to non-intercalative binding mode, most likely aggregation of **32** and **25** molecules along the polynucleotide backbone and inside the grooves. At excess of **10**, **6**, **37** and **30** over polynucleotide binding sites, compounds form aggregates along DNA double helix. Moderate to high binding affinities ($\log K_s$ =5-7) obtained for selected imidazo[4,5-*b*]pyridine derivatives suggest that DNA/RNA are potential cell targets. Nevertheless, since high binding affinities were noticed even in the case of low antiproliferative activity (like with **37**), targets other than DNA and RNA could also be involved in the mechanism of biological action.

3. Experimental part

3.1. General methods

All chemicals and solvents were purchased from commercial suppliers Aldrich and Acros. Melting points were recorded on SMP11 Bibby and Büchi 535 apparatus. All NMR spectra were measured in DMSO-d_6 solutions using TMS as an internal standard. The ^{1}H and ^{13}C NMR spectra were recorded on a Varian Bruker Avance III HD 400 MHz/54 mm Ascend. Chemical shifts are reported in ppm (δ) relative to TMS. All compounds were routinely checked by TLC with Merck silica gel 60F-254 glass plates. The microwave-assisted synthesis was performed in a Milestone start S microwave oven using quartz cuvettes under the pressure of 40 bar. Elemental analysis for carbon, hydrogen and nitrogen were performed on a Perkin-Elmer 2400 elemental analyzer. Where analyses are indicated only as symbols of elements, analytical results obtained are within 0.4% of the theoretical value. Mass spectra were recorded on Agilent 1200 Series HPLC system with an Agilent 6420 DAD mass detector and a triple quadrupole mass spectrometer.

3.2. Synthesis

3.2.1. Synthesis of 2-amino substituted pyrido[3',2':4,5]imidazo[1,2-*a*]quinoline-6-carbonitriles and pyrido[2',3':4,5]imidazo[1,2-*a*]quinoline-6-carbonitriles

2-(1H-imidazo[4,5-b]pyridin-2-yl)acetonitrile ***2***

A mixture of equimolar amounts of 2,3-diaminopyridine (2.800 g, 25.70 mmol) and 2-cyanoacetamide (4.310 g, 25.70 mmol) was heated in an oil bath for 20 min at 190 °C. After cooling, the reaction mixture was recrystallized from 50% ethanol/water (130 mL) to obtain a light brown powder (3.420 g, 84%); mp 268–271 °C; ^{1}H NMR (300 MHz, DMSO-d_6): δ/ppm = 13.06 (bs, 1H, NH), 8.34 (s, 1H, H_{arom}), 8.00 (s, 1H, H_{arom}), 7.25 (dd, 1H, J_1 = 8.03 Hz, J_2 = 4.79 Hz, H_{arom}), 4.42 (s, 2H, CH_2); ^{13}C NMR (75 MHz, DMSO-d_6): δ/ppm = 144.3, 118.6 (2C), 19.2; MS (ESI) m/z 159.0 $[M+H]^+$.

(E)-3-(2-chloro-4-fluorophenyl)-2-(1H-imidazo[4,5-b]pyridin-2-yl)acrylonitrile ***4***

Compound **4** was prepared from 2-(1*H*-imidazo[4,5-*b*]pyridin-2-yl)acetonitrile **2** (1.000 g, 6.27 mmol), 2-chloro-4-fluorobenzaldehyde **3**, few drops of piperidine in absolute ethanol (10 mL) after refluxing for 1.5 h and recrystallization from ethanol to yield 1.080 g (58%) of yellow powder; mp 246–249 °C; ^{1}H NMR (300 MHz, DMSO-d_6): δ/ppm = 13.91 (s, 1H, NH), 8.55 (s, 1H, H_{arom}), 8.44 (d, 1H, J = 3.75 Hz, H_{arom}), 8.22 (dd, 1H, J_1 = 8.76 Hz, J_2 =

6.09 Hz, H_{arom}), 8.12 (d, 1H, J = 7.05 Hz, H_{arom}), 7.75 (dd, 1H, J_1 = 8.76 Hz, J_2 = 2.58 Hz, H_{arom}), 7.52 (td, 1H, J_1 = 8.57 Hz, J_2 = 2.59 Hz, H_{arom}), 7.33 (dd, 1H, J = 8.07 Hz, J_2 = 4.77 Hz, H_{arom}); ^{13}C NMR (75 MHz, DMSO-d_6): δ/ppm = 163.8 (d, J_{CF} = 256.02 Hz), 157.8, 144.4, 142.2, 135.9, 135.7, 132.2 (d, J_{CF} = 9.00 Hz), 128.3, 118.4 (d, J_{CF} = 25.50 Hz), 116.0 (d, J_{CF} = 21.10 Hz), 115.5; Found: C, 60.06; H, 2.93; N, 18.50. Calc. for $C_{15}H_8ClFN_4$: C, 60.32; H, 2.70; N, 18.76%; MS (ESI) m/z 299.0 $[M+H]^+$.

*2-fluoropyrido[3',2':4,5]imidazo[1,2-a]quinoline-6-carbonitrile 5a and 2-fluoropyrido-[2',3':4,5]imidazo[1,2-a]quinoline-6-carbonitrile **5b***

Compound **4** (0.840 g, 2.81 mmol) was dissolved in 6.5 ml of sulfolane and the reaction mixture was heated for 25 minutes at 280 °C. The cooled mixture was poured into water (15 ml) and the resulting product was filtered off. Brown powder product (0.711 g) was obtained in the form of a mixture of regioisomers in the ratio **5a:5b** = 1:1 separated by column chromatography on SiO_2 using CH_2Cl_2/methanol as eluent.

*2-fluoropyrido[3',2':4,5]imidazo[1,2-a]quinoline-6-carbonitrile **5a***

There was obtained 0.201 g (27%) of a yellow powder product **5a**. mp 290–292 °C; ^{1}H NMR (300 MHz, DMSO-d_6): δ/ppm = 9.41 (dd, 1H, J_1 = 10.77 Hz, J_2 = 2.52 Hz, H_{arom}), 8.84 (s, 1H, H_{arom}), 8.68 (dd, 1H, J_1 = 4.71 Hz, J_2 = 1.44 Hz, H_{arom}), 8.43 (dd, 1H, J_1 = 8.19 Hz, J_2 = 1.44 Hz, H_{arom}), 8.19 (dd, 1H, J_1 = 8.85 Hz, J_2 = 6.24 Hz, H_{arom}), 7.68 (dd, 1H, J = 8.19 Hz, J_2 = 4.71 Hz, H_{arom}), 7.56 (td, 1H, J_1 = 8.61 Hz, J_2 = 2.59 Hz, H_{arom}); ^{13}C NMR (75 MHz, DMSO-d_6): δ/ppm = 164.9 (d, J_{CF} = 250.71 Hz), 145.1, 144.6, 141.8, 136.8, 136.7, 136.5, 133.9 (d, J_{CF} = 10.73 Hz), 128.7, 121.8, 118.4, 115.4, 114.7 (d, J_{CF} = 23.36 Hz), 104.3 (d, J_{CF} = 28.62 Hz), 100.9; Found: C, 68.52; H, 2.80; N, 21.20. Calc. for $C_{15}H_7FN_4$: C, 68.70; H, 2.69; N, 21.36%; MS (ESI) m/z 263.0 $[M+H]^+$.

*2-fluoropyrido[2',3':4,5]imidazo[1,2-a]quinoline-6-carbonitrile **5b***

There was obtained 0.148 g (20%) of a yellow powder product **5b**. mp >300 °C; ^{1}H NMR (300 MHz, DMSO-d_6): δ/ppm = 9.29 (dd, 1H, J_1 = 8.40 Hz, J_2 = 1.08 Hz, H_{arom}), 8.97 (s, 1H, H_{arom}), 8.80 (dd, 1H, J_1 = 4.56 Hz, J_2 = 1.02 Hz, H_{arom}), 8.65 (dd, 1H, J_1 = 10.37 Hz, J_2 = 2.09 Hz, H_{arom}), 8.30 (dd, 1H, J_1 = 8.78 Hz, J_2 = 6.38 Hz, H_{arom}), 7.69 – 7.56 (m, 2H, H_{arom});^{13}C NMR (75 MHz, DMSO-d_6): δ/ppm = 165.4 (d, J_{CF} = 258.09 Hz), 147.9, 141.9, 134.8 (d, J_{CF} = 10,99 Hz), 123.9, 123.7, 118.9, 118.7, 115.6, 114.7 (d, J_{CF} = 23,34 Hz), 104.1 (d, J_{CF} = 27,60 Hz), 100.8, 97.6; Found: C, 68.59; H, 2.72; N, 21.29. Calc. for $C_{15}H_7FN_4$: C, 68.70; H, 2.69; N, 21.36%; MS (ESI) m/z 263.0 $[M+H]^+$.

3.2.1.1. General method for preparation of compounds 6-13

Compounds **6-13** were prepared using microwave irradiation, at optimized reaction time at 170 °C with power 800 W and 40 bar pressure, from compound **5a** or **5b** in acetonitrile (10 mL) with an excess of added corresponding amine. After cooling, the reaction mixture was filtered off and the resulting product was separated by column chromatography on SiO_2 using dichloromethane/methanol as eluent.

*2-[(3-(N,N-dimethylamino)propyl)amino]pyrido[3',2':4,5]imidazo[1,2-a]quinoline-6-carbonitrile **6***

Compound **6** was prepared using above described method from **5a** (0.120 mg, 0.46 mmol) and *N,N*-dimethylaminopropyl-1-amine (0.40 mL, 3.92 mmol) after 10 h of irradiation to yield 0.070 mg (45%) of yellow powder; mp 245–248 °C; ^{1}H NMR (300 MHz, DMSO-d_6): δ/ppm = 8.92 (d, 1H, J = 1.83 Hz, H_{arom}), 8.60 (dd, 1H, J_1 = 4.71 Hz, J_2 = 1.41 Hz, H_{arom}), 8.53 (s, 1H, H_{arom}), 8.33 (dd, 1H, J_1 = 8.87 Hz, J_2 = 1.41 Hz, H_{arom}), 7.78 (d, 1H, J = 8.88 Hz, H_{arom}), 7.63 – 7.59 (m, 2H, H_{arom}), 6.93 (dd, 1H, J_1 = 8.85 Hz, J_2 = 2.16 Hz, H_{arom}), 3.30 – 3.23 (m, 2H, CH_2), 2.56 (t, 2H, J = 1.74 Hz, CH_2), 2.31 (s, 6H, CH_3), 1.92 – 1.81 (m, 2H, CH_2); ^{13}C NMR (150 MHz, DMSO-d_6): δ/ppm= 153.9, 146.1, 145.2, 142.5, 141.2, 136.4, 126.8, 120.6, 116.5, 111.0, 91.5, 56.3, 44.6 (2C), 40.6, 25.6; Found: C, 69.42; H, 5.98; N, 24.60. Calc. for $C_{20}H_{20}N_6$: C, 69.75; H, 5.85; N, 24.40%; MS (ESI) m/z 345.1 $[M+H]^+$.

2-(N-isobutylamino)pyrido[3',2':4,5]imidazo[1,2-a]quinoline-6-carbonitrile 7

Compound **7** was prepared using above described method from **5a** (0.080 mg, 0.30 mmol) and isobutylamine (0.15 mL, 1.42 mmol) after 4 h of irradiation to yield 0.052 mg (54%) of yellow powder; mp 224–227 °C; ^{1}H NMR (300 MHz, DMSO-d_6): δ/ppm = 8.96 (d, 1H, J = 1.95 Hz, H_{arom}), 8.61 (dd, 1H, J_1 = 1.46 Hz, J_2 = 4.73 Hz, H_{arom}), 8.53 (s, 1H, H_{arom}), 8.33 (dd, 1H, J_1 = 1.44 Hz, J_2 = 8.16 Hz, H_{arom}), 7.78 (d, 1H, J = 8.88 Hz, H_{arom}), 7.65 (t, 1H, J = 4.74 Hz, NH_{amine}), 7.61 (dd, 1H, J_1 = 4.71 Hz, J_2 = 8.13 Hz, H_{arom}), 6.96 (dd, 1H, J_1 = 2.18 Hz, J_2 = 8.87 Hz, H_{arom}), 3.31 (t, 2H, J = 6.17 Hz, CH_2), 2.06 – 1.97 (m, 1H, CH), 1.03 (d, 6H, J = 6.63 Hz, CH_3); ^{13}C NMR (150 MHz, DMSO-d_6): δ/ppm = 154.2, 146.2, 145.2, 142.5, 141.2, 136.4, 126.9, 120.6, 116.5, 110.9, 91.4, 50.3, 27.3, 20.3 (2C); Found: C, 72.23; H, 5.63; N, 22.14. Calc. for $C_{19}H_{17}N_5$: C, 72.36; H, 5.43; N, 22.21%; MS (ESI) m/z 314.1 $[M+H]^+$.

*2-(N-piperidin-1-yl)pyrido[3',2':4,5]imidazo[1,2-a]quinoline-6-carbonitrile **8***

Compound **8** was prepared using above described method from **5a** (0.080 mg, 0.30 mmol)

and piperidine (0.21 mL, 2.13 mmol) after 4 h of irradiation to yield 0.041 mg (51%) of yellow powder; mp 262–265 °C; ^{1}H NMR (300 MHz, DMSO-d_6): δ/ppm = 9.26 (d, 1H, J = 2.16 Hz, H_{arom}), 8.65 (dd, 1H, J_1 = 4.73 Hz, J_2 = 1.43 Hz, H_{arom}), 8.59 (s, 1H, H_{arom}), 8.36 (dd, 1H, J_1 = 8.18 Hz, J_2 = 1.43 Hz, H_{arom}), 7.87 (d, 1H, J = 9.15 Hz, H_{arom}), 7.62 (dd, 1H, J_1 = 8.16 Hz, J_2 = 4.74 Hz, H_{arom}), 7.30 (dd, 1H, J = 9.12 Hz, J_2 = 2.40 Hz, H_{arom}), 3.63 (bs, 4H, CH_2), 1.70 (bs, 6H, CH_2); ^{13}C NMR (75 MHz, DMSO-d_6): δ/ppm = 154.5, 143.4, 141.5, 138.1, 132.4, 127.8, 127.6, 121.2, 116.8, 113.2, 111.9, 99.2, 48.3 (2C), 25.5 (2C), 24.4; Found: C, 73.19; H, 5.43; N, 21.38. Calc. for $C_{20}H_{17}N_5$: C, 73.37; H, 5.23; N, 21.39%; MS (ESI) m/z 328.1 $[M+H]^+$.

*2-(N-piperazin-1-yl)pyrido[3',2':4,5]imidazo[1,2-a]quinoline-6-**carbonitrile 9***

Compound **9** was prepared using above described method from **5a** (0.120 mg, 0.46 mmol) and piperazine (0.260 mg, 3.02 mmol) after 10 h of irradiation to yield 0.068 mg (45%) of yellow powder; mp 244–247 °C; ^{1}H NMR (300 MHz, DMSO-d_6): δ/ppm = 9.25 (d, 1H, J = 2.07 Hz, H_{arom}), 8.65 (dd, 1H, J_1 = 4.71 Hz, J_2 = 1.44 Hz, H_{arom}), 8.62 (s, 1H, H_{arom}), 8.37 (dd, 1H, J_1 = 8.15 Hz, J_2 = 1.40 Hz, H_{arom}), 7.90 (d, 1H, J = 9.15 Hz, H_{arom}), 7.64 (dd, 1H, J_1 = 8.16 Hz, J_2 = 4.74 Hz, H_{arom}), 7.32 (dd, 1H, J_1 = 9.11 Hz, J_2 = 2.36 Hz, H_{arom}), 3.58 (t, 4H, J = 4.89 Hz, CH_2), 3.02 (t, 4H, J = 4.88 Hz, CH_2); ^{13}C NMR (75 MHz, DMSO-d_6): δ/ppm = 154.7, 146.1, 145.5, 143.5, 141.5, 137.9, 136.8, 132.3, 127.8, 121.3, 116.6, 113.3, 112.6, 99.5, 94.5, 47.3 (2C), 45.1 (2C); Found: C, 69.26; H, 5.04; N, 25.70. Calc. for $C_{19}H_{16}N_6$: C, 69.50; H, 4.91; N, 25.59%; MS (ESI) m/z 329.1 $[M+H]^+$.

2-[(3-(N,N-dimethylamino)propyl)amino]pyrido[2',3':4,5]imidazo[1,2-a]quinoline-6-*carbonitrile **10***

Compound **10** was prepared using above described method from **5b** (0.045 mg, 0.17 mmol) and *N,N*-dimethylaminopropyl-1-amine (0.15 mL, 1.20 mmol) after 5 h of irradiation to yield 0.031 mg (53%) of yellow powder; mp 250–254 °C**;** ^{1}H NMR (300 MHz, DMSO-d_6): δ/ppm = 8.90 (t, 1H, J = 5.19 Hz, NH_{arom}), 8.72 – 8.68 (m, 1H, H_{arom}), 8.54 (s, 1H, H_{arom}), 7.88 – 7.74 (m, 2H, H_{arom}), 7.55 – 7.48 (m, 2H, H_{arom}), 7.00 – 7.88 (m, 1H, H_{arom}), 3.66 (bs, 2H, CH_2), 3.45 (bs, 2H, CH_2), 3.29 (s, 6H, CH_3), 2.20 (bs, 2H, CH_2); ^{13}C NMR (75 MHz, DMSO-d_6): δ/ppm = 155.9, 154.8, 154.3, 147.7, 147.1, 141.5, 133.3, 123.3, 123.0, 122.9, 117.7, 116.9, 111.8, 92.2, 67.2, 56.9, 45.5 (2C), 22.9; Found: C, 69.79; H, 5.71; N, 24.50. Calc. for $C_{20}H_{20}N_6$: C, 69.75; H, 5.85; N, 24.40%; MS (ESI) m/z 345.1 $[M+H]^+$.

*2-(N-isobutylamino)pyrido[2',3':4,5]imidazo[1,2-a]quinoline-6-carbonitrile **11***

Compound **11** was prepared using above described method from **5b** (0.080 mg, 0.30 mmol) and isobutylamine (0.15 mL, 1.52 mmol) after 4 h of irradiation to yield 0.056 mg (70%) of yellow powder; mp 289–291 °C; ^{1}H NMR (300 MHz, DMSO-d_6): δ/ppm = 8.87 (dd, 1H, J_1 = 8.21 Hz, J_2 = 1.01 Hz, H_{arom}), 8.72 (dd, 1H, J_1 = 4.67 Hz, J_2 = 1.01 Hz, H_{arom}), 8.57 (s, 1H, H_{arom}), 7.84 (d, 1H, J = 8.91 Hz, H_{arom}), 7.69 (Bs, 1H, H_{arom}), 7.54 (dd, 1H, J_1 = 8.34 Hz, J_2 = 4.74 Hz, H_{arom}), 7.45 (t, 1H, J = 5.04 Hz, NH_{amin}), 6.99 (dd, 1H, J_1 = 8.93 Hz, J_2 = 1.40 Hz, H_{arom}), 3.17 (t, 2H, J = 6.15 Hz, CH_2), 2.01 – 1.90 (m, 1H, CH), 1.03 (d, 6H, J = 6.63 Hz, CH_3); ^{13}C NMR (75 MHz, DMSO-d_6): δ/ppm = 155.8, 154.4, 147.5, 146.6, 141.1, 133.2, 122.9, 122.3, 117.2, 116.6, 111.2, 91.3, 49.9, 27.6, 20.3 (2C); Found: C, 72.49; H, 5.21; N, 22.30. Calc. for $C_{19}H_{17}N_5$: C, 72.36; H, 5.43; N, 22.21%; MS (ESI) m/z 316.1 $[M+H]^+$.

*2-(N-piperidin-1-yl)pyrido[2',3':4,5]imidazo[1,2-a]quinoline-6-carbonitrile **12***

Compound **12** was prepared using above described method from **5b** (0.080 mg, 0.30 mmol) and piperidine (0.21 mL, 2.13 mmol) after 4 h of irradiation to yield 0.049 mg (61%) of yellow powder; mp 290–293 °C; ^{1}H NMR (300 MHz, DMSO-d_6): δ/ppm = 8.91 (d, 1H, J = 8.37 Hz, H_{arom}), 8.73 (d, 1H, J = 4.62 Hz, H_{arom}), 8.62 (s, 1H, H_{arom}), 7.90 (d, 1H, J = 7.35 Hz, H_{arom}), 7.64 (s, 1H, H_{arom}), 7.52 (dd, 1H, J_1 = 8.30 Hz, J_2 = 4.70 Hz, H_{arom}), 7.33 (d, 1H, J = 9.18 Hz, H_{arom}), 3.67 (s, 4H, CH_2), 1.70 (s, 6H, CH_2); ^{13}C NMR (75 MHz, DMSO-d_6): δ/ppm = 155.9, 154.6, 147.9, 147.3, 141.2, 138.7, 133.2, 123.6, 123.3, 118.1, 116.8, 113.4, 112.2, 97.4, 93.5, 48.5 (2C), 25.5 (2C), 24.3; Found: C, 73.29; H, 5.31; N, 21.40. Calc. for $C_{20}H_{17}N_5$: C, 73.37; H, 5.23; N, 21.39%; MS (ESI) m/z 328.1 $[M+H]^+$.

*2-(N-piperazin-1-yl)pyrido[2',3':4,5]imidazo[1,2-a]quinoline-6-carbonitrile **13***

Compound **13** was prepared using above described method from **5b** (0.040 mg, 015 mmol) and piperazine (0.150 mg, 1.74 mmol) after 5 h of irradiation to yield 0.028 mg (55%) of yellow powder; mp >300 °C; ^{1}H NMR (300 MHz, DMSO-d_6): δ/ppm = 8.97 (d, 1H, J = 8.39 Hz, H_{arom}), 8.75 – 8.74 (m, 1H, H_{arom}), 8.66 (s, 1H, H_{arom}), 7.97 (d, 1H, J = 8.98 Hz, H_{arom}), 7.69 (bs, 1H, H_{arom}), 7.52 (dd, 1H, J_1 = 8.10 Hz, J_2 = 4.62 Hz, H_{arom}), 7.36 (d, 1H, J = 8.90 Hz, H_{arom}), 3.83 (bs, 4H, CH_2), 3.62 (bs, 4H, CH_2); ^{13}C NMR (100 MHz, DMSO-d_6): δ/ppm = 162.6, 154.0, 147.5, 141.4, 138.3, 133.3, 132.1, 123.8, 123.3, 118.2, 116.5, 113.5, 113.4, 98.6, 95.2, 45.0 (2C), 43.5 (2C); Found: C, 69.66; H, 4.88; N, 25.46. Calc. for $C_{19}H_{16}N_6$: C, 69.50; H, 4.91; N, 25.59%; MS (ESI) m/z 329.1 $[M+H]^+$.

4.2.2. Synthesis of 5-amino substituted pyrido[3',2':4,5]imidazo[1,2-*a*]quinoline-6-carbonitriles and pyrido[2',3':4,5]imidazo[1,2-*a*]quinoline-6-carbonitriles

*(Z)-3-(2-chlorophenyl)-3-hydroxy-2-(3H-imidazo[4,5-b]pyridin-2-yl)acrylonitrile **16***

A solution of 1.000 g (6.32 mmol) 2-(1*H*-imidazo[4,5-*b*]pyridin-2-yl)acetonitrile **2** and 0.80 mL (6.32 mmol) 2-chlorobenzoylchloride **14** in pyridine (7 mL) was refluxed for 1.5 h. The cooled mixture was poured into water (50 mL) and the resulting product was filtered off and recrystallized from ethanol to obtain an orange powder (1.240 g, 66%); mp >300 °C; ^{1}H NMR (300 MHz, DMSO-d_6): δ/ppm = 13.81 (bs, 1H, OH), 13.29 (bs, 1H, $H_{imidazopiridin}$), 8.28 (dd, 1H, J_1= 5.22 Hz, J_2 = 1.23 Hz, H_{arom}), 7.97 (dd, 1H, J_1 = 7.88 Hz, J_2 = 1.16 Hz, H_{arom}), 7.52 (dd, 1H, J_1 = 7.68 Hz, J_2 = 2.01 Hz, H_{arom}), 7.48 – 7.40 (m, 3H, H_{arom}), 7.32 (dd, 1H, J_1 = 7.91 Hz, J_2 = 5.27 Hz, H_{arom}); ^{13}C NMR (75 MHz, DMSO-d_6): δ/ppm = 186.5, 154.0, 149.2, 140.9, 130.8, 129.9, 129.9, 128.8, 127.5, 121.1, 120.0, 118.6, 64.5; Found: C, 60.59; H, 3.35; N, 18.70. Calc. for $C_{15}H_9ClN_4O$: C, 60.72; H, 3.06; N, 18.88%; MS (ESI) m/z 297.0 $[M+H]^+$.

*5-oxo-5,7-dihydropyrido[3',2':4,5]imidazo[1,2-a]quinoline-6-carbonitrile 18a and 5-oxo-5,7-dihydropyrido[2',3':4,5]imidazo[1,2-a]quinoline-6-carbonitrile **18b***

A solution of 1.192 g (4.01 mmol) (*Z*)-3-(2-chlorophenyl)-3-hydroxy-2-(3*H*-imidazo[4,5-*b*]pyridin-2-yl)acrylonitrile **16** and 1.125 g *t*-KOBu in DMF (14 mL) was refluxed for 2 h. After cooling, the reaction mixture was evaporated under vacuum and dissolved in water (50 mL). The resulting product was filtered off and recrystallized from ethanol to obtain a brown powder (0.759 g, 73%) in the form of a mixture of regioisomers in the ratio **18a:18b** = 1:5; mp >300 °C; **18a**: ^{1}H NMR (300 MHz, DMSO-d_6): δ/ppm = 9.64 (d, 1H, J = 8.01 Hz, H_{arom}), 8.37 (dd, 1H, J_1 = 4.67 Hz, J_2 = 1.16 Hz, H_{arom}), 8.28 – 8.23 (m, 1H, H_{arom}), 7.90 (dd, 1H, J_1 = 6.08 Hz, J_2 = 1.37 Hz, H_{arom}), 7.77 (d, 1H, J = 1.17 Hz, H_{arom}), 7.57 – 7.55 (m, 1H, H_{arom}), 7.45 (dd, 1H, J_1 = 7.92 Hz, J_2 = 5.19 Hz, H_{arom}); **18b**: ^{1}H NMR (300 MHz, DMSO-d_6): δ/ppm = 8.82 (d, 1H, J = 8.04 Hz, H_{arom}), 8.49 (d, 1H, J = 8.37 Hz, H_{arom}), 8.35 – 8.37 (m, 2H, H_{arom}), 7.85 (td, 1H, J_1 = 7.70 Hz, J_2 = 1.50 Hz, H_{arom}), 7.55 (t, 1H, J = 7.49 Hz, H_{arom}), 7.31 (dd, 1H, J_1 = 8.13 Hz, J_2 = 5.43 Hz, H_{arom}); MS (ESI) m/z 261.1 $[M+H]^+$.

*5-chloropyrido[3',2':4,5]imidazo[1,2-a]quinoline-6-carbonitrile 20 and 5-chloropyrido-[2',3':4,5]imidazo[1,2-a]quinoline-6-carbonitrile **22***

A solution of 0.500 g (1.92 mmol) 5-oxo-5,7-dihydropyrido[3',2':4,5]imidazo[1,2-*a*]quinoline-6-carbonitrile **18a** and 5-oxo-5,7-dihydropyrido[2',3':4,5]imidazo[1,2-*a*]quinoline-6-carbonitrile **18b**, 0.214 g PCl_5 in $POCl_3$ (11 mL) was refluxed for 1.5 h. After cooling, the reaction mixture was evaporated under vacuum and dissolved in water (10 ml). The resulting product was filtered off and washed with water to obtain a yellow powder (0.373 g, 78%) in the form of a mixture of regioisomers in the ratio **20:22** = 1:5 separated by

column chromatography on SiO_2 using CH_2Cl_2/methanol as eluent.

20: 0.027 g, mp >300 °C; ^{1}H NMR (300 MHz, DMSO-*d*$_6$): δ/ppm = 9.94 (d, 1H, *J* = 8.34 Hz, H_{arom}), 8.74 (d, 1H, *J* = 4.23 Hz, H_{arom}), 8.49 (d, 1H, *J* = 7.20 Hz, H_{arom}), 8.40 (d, 1H, *J* = 8.49 Hz, H_{arom}), 8.18 (t, 1H, *J* = 7.13 Hz, H_{arom}), 7.82 (t, 1H, *J* = 7.91 Hz, H_{arom}), 7.72 (t, 1H, *J* = 6.37 Hz, H_{arom}); ^{13}C NMR (75 MHz, DMSO-*d*$_6$): δ/ppm = not enough soluble; Found: C, 64.52; H, 2.41; N, 20.36. Calc. for $C_{15}H_7ClN_4$: C, 64.65; H, 2.53; N, 20.10%; MS (ESI) m/z 279.0 $[M+H]^+$.

22: 0.249 g, mp >300 °C; ^{1}H NMR (300 MHz, DMSO-*d*$_6$): δ/ppm = 9.17 (dd, 1H, J_1 = 8.48 Hz, J_2 = 1.20 Hz, H_{arom}), 8.86 (d, 1H, *J* = 8.49 Hz, H_{arom}), 8.79 (dd, 1H , J_1 = 4.67 Hz, J_2 = 1.22 Hz, H_{arom}), 8.40 (dd, 1H, J_1 = 8.19, J_2 = 1.26 Hz, H_{arom}), 8.10 (td, 1H, J_1 = 7.89 Hz, J_2 = 1.32 Hz, H_{arom}), 7.80 (t, 1H, *J* = 7.71 Hz, H_{arom}), 7.60 (dd, 1H, J_1 = 8.43 Hz, J_2 = 4.68 Hz, H_{arom}); ^{13}C NMR (75 MHz, DMSO-*d*$_6$): δ/ppm = 152.9, 151.4, 149.9, 148.9, 139.0, 136.4, 132.4, 129.6, 129.5, 127.6, 124.8, 123.3, 120.05, 119.3, 117.9; Found: C, 64.72 H, 2.33; N, 20.26. Calc. for $C_{15}H_7ClN_4$: C, 64.65; H, 2.53; N, 20.10%; MS (ESI) m/z 279.0 $[M+H]^+$.

4.2.2.2. General method for preparation of compounds 24-27 and 31-34

Compounds **24-27** and **31-34** were prepared using microwave irradiation, at optimized reaction time at 170 °C with power 800 W and 40 bar pressure, from compound **20** or **22** in acetonitrile (10 mL) with an excess of added corresponding amine. After cooling, the reaction mixture was filtered off and the resulting product was separated by column chromatography on SiO_2 using dichloromethane/methanol as eluent.

*5-[(3-(N,N-dimethylamino)propyl)amino]pyrido[3',2':4,5]imidazo[1,2-a]quinoline-6-carbonitrile **24***

Compound **24** was prepared using above described method from **20** (0.070 mg, 0.20 mmol) and *N,N*-dimethylaminopropyl-1-amine (0.16 mL, 1.00 mmol) after 4 h of irradiation to yield 0.047 mg (69%) of yellow powder; mp 211–213 °C; ^{1}H NMR (600 MHz, DMSO-*d*$_6$): δ/ppm = 9.69 (dd, 1H, J_1 = 8.40 Hz, J_2 = 0.84 Hz, H_{arom}), 8.74 (bs, 1H, NH_{amin}), 8.33 (dd, 1H, J_1 = 4.74 Hz, J_2 = 1.44 Hz, H_{arom}), 8.13 (d, 1H, *J* = 7.92 Hz, H_{arom}), 8.05 (dd, 1H, J_1 = 8.01 Hz, J_2 = 1.41 Hz, H_{arom}), 7.85 (td, 1H, J_1 = 8.19 Hz, J_2 = 0.90 Hz, H_{arom}), 7.52 (td, 1H, J_1 = 8.19 Hz, J_2 = 0.99 Hz, H_{arom}), 7.41 (dd, 1H, J_1 = 7.95 Hz, J_2 = 4.77 Hz, H_{arom}), 3.92 (s, 2H, CH_2), 2.43 (t, 2H, *J* = 6.45 Hz, CH_2), 2.21 (s, 6H, CH_3), 1.89 (p, 2H, *J* = 6.66 Hz, CH_2); ^{13}C NMR (150 MHz, DMSO-*d*$_6$): δ/ppm = 151.5, 149.9, 146.6, 141.1, 137.5, 134.9, 133.1, 125.6, 125.4, 123.9, 120.2, 117.9, 117.6, 116.8, 71.7, 57.5, 45.5 (2C), 44.4, 26.7; Found: C, 69.62; H, 5.78;

N, 24.60. Calc. for $C_{20}H_{20}N_6$: C, 69.75; H, 5.85; N, 24.40%; MS (ESI) m/z 345.1 $[M+H]^+$.

5-(N-isobutylamino)pyrido[3',2':4,5]imidazo[1,2-a]quinoline-6-carbonitrile ***25***

Compound **25** was prepared using above described method from **20** (0.080 mg, 0.29 mmol) and isobutylamine (0.15 mL, 1.42 mmol) after 4 h of irradiation to yield 0.053 mg (54%) of orange powder; mp 250–252 °C; ^{1}H NMR (300 MHz, DMSO-d_6): δ/ppm = 9.80 (dd, 1H, J_1 = 8.43 Hz, J_2 = 0.96 Hz, H_{arom}), 8.50 (d, 1H, J = 7.89 Hz, H_{arom}), 8.39 (dd, 1H, J_1 = 4.82 Hz, J_2 = 1.43 Hz, H_{arom}), 8.37 (bs, 1H, NH_{amin}), 8.10 (dd, 1H, J_1 = 8.01 Hz, J_2 = 1.41 Hz, H_{arom}), 7.95 (td, 1H, J_1 = 7.83 Hz, J_2 = 1.41 Hz, H_{arom}), 7.61 (td, 1H, J_1 = 7.74 Hz, J_2 = 0.87 Hz, H_{arom}), 7.46 (dd, 1H, J_1 = 8.01 Hz, J_2 = 4.83 Hz, H_{arom}), 3.69 (t, 2H, J = 6.69 Hz, CH_2), 2.28-2.12 (m, 1H, CH), 1,01 (d, 6H, J = 6.63 Hz, CH_3); ^{13}C NMR (75 MHz, DMSO-d_6): δ/ppm = 151.2, 149.8, 146.5, 141.1, 137.4, 134.95, 133.4, 125.7, 125.4, 124.3, 120.3, 117.8, 117.7, 116.7, 71.7, 51.4, 28.7, 19.9 (2C); Found: C, 72.17; H, 5.31; N, 22.52. Calc. for $C_{19}H_{17}N_5$: C, 72.36; H, 5.43; N, 22.21%; MS (ESI) m/z 316.1 $[M+H]^+$.

5-(N-piperidin-1-yl)pyrido[3',2':4,5]imidazo[1,2-a]quinoline-6-carbonitrile ***26***

Compound **26** was prepared using above described method from **20** (0.080 mg, 0.29 mmol) and piperidine (0.21 mL, 2.13 mmol) after 4 h of irradiation to yield 0.037 mg (39%) of orange powder; mp 240–243 °C; ^{1}H NMR (600 MHz, DMSO-d_6): δ/ppm = 9.84 (dd, 1H, J_1 = 8.43 Hz, J_2 = 1.05 Hz, H_{arom}), 8.54 (dd, 1H, J_1 = 4.71 Hz, J_2 = 1.47 Hz, H_{arom}), 8.27 (dd, 1H, J_1 = 8.07 Hz, J_2 = 1.47 Hz, H_{arom}), 8.12 (dd, 1H, J_1 = 8.25 Hz, J_2 = 1.29 Hz, H_{arom}), 7.99 (td, 1H, J_1 = 7.80 Hz, J_2 = 1.41 Hz, H_{arom}), 7.65 (td, 1H, J_1 = 7.71 Hz, J_2 = 1.17 Hz, H_{arom}), 7.56 (dd, 1H, J_1 = 8.07 Hz, J_2 = 4.71 Hz, H_{arom}), 3.63 (t, 4H, J = 5.28 Hz, CH_2), 1.86 – 1.82 (m, 4H, CH_2), 1.76 – 1.73 (m, 2H, CH_2); ^{13}C NMR (75 MHz, DMSO-d_6): δ/ppm = 159.7, 142.8, 137.0, 136.0, 133.6, 127.6, 127.1, 125.6, 120.9, 119.8, 117.9, 116.4, 54.4 (2C), 26.5 (2C), 23.9; Found: C, 73.22; H, 5.49; N, 21.29. Calc. for $C_{20}H_{17}N_5$: C, 73.37; H, 5.23; N, 21.39%; MS (ESI) m/z 328.1 $[M+H]^+$.

5-(N-piperazin-1-yl)pyrido[3',2':4,5]imidazo[1,2-a]quinoline-6-carbonitrile ***27***

Compound **27** was prepared using above described method from **20** (0.070 mg, 0.20 mmol) and piperazine (0.108 mg, 1.30 mmol) after 4 h of irradiation to yield 0.057 mg (71%) of yellow powder; mp 274–276 °C; ^{1}H NMR (300 MHz, DMSO-d_6): δ/ppm = 9.79 (d, 1H, J = 7.83 Hz, H_{arom}), 8.53 (dd, 1H, J_1 = 4.76 Hz, J_2 = 1.40 Hz, H_{arom}), 8.27 (dd, 1H, J_1 = 8.09 Hz, J_2 = 1.40 Hz, H_{arom}), 8.13 (dd, 1H, J_1 = 8.28 Hz, J_2 = 0.72 Hz, H_{arom}), 7.96 (td, 1H, J_1 = 7.80 Hz, J_2 = 1.10 Hz, H_{arom}), 7.62 (td, 1H, J_1 = 7.70 Hz, J_2 = 0.89 Hz, H_{arom}), 7.56 (dd, 1H, J_1 =

8.10 Hz, J_2 = 4.77 Hz, H_{arom}), 3.58 (t, 4H, J = 4.64 Hz, CH_2), 3.00 (t, 4H, J = 4.65 Hz, CH_2), 2.08 (s, 1H, NH); ^{13}C NMR (75 MHz, DMSO-d_6): δ/ppm = 159.1, 155.7, 148.0, 142.8, 137.0, 136.0, 133.5, 128.5, 127.7, 127.2, 125.6, 120.9, 119.6, 117.8, 116.3, 54.3 (2C), 46.4 (2C); Found: C, 69.29; H, 4.75; N, 25.96. Calc. for $C_{19}H_{16}N_6$: C, 69.50; H, 4.91; N, 25.59%; MS (ESI) m/z 329.1 $[M+H]^+$.

5-((3-(N,N-dimethylamino)propyl)amino)pyrido[2',3':4,5]imidazo[1,2-a]quinoline-6-carbonitrile ***31***

Compound **31** was prepared using above described method from **22** (0.070 mg, 0.20 mmol) and *N,N*-dimethylaminopropyl-1-amine (0.16 mL, 1.00 mmol) after 4 h of irradiation to yield 0.047 mg (69%) of yellow powder; mp 253–255 °C; ^{1}H NMR (300 MHz, DMSO-d_6): δ/ppm = 8.85 (s, 1H, NH_{amin}), 8.77 (dd, 1H, J_1 = 8.25 Hz, J_2 = 1.21 Hz, H_{arom}), 8.58 (d, 1H, J = 8.33 Hz, H_{arom}), 8.50 (dd, 1H, J_1 = 4.81 Hz, J_2 = 1.11 Hz, H_{arom}), 8.25 (d, 1H, J = 7.61 Hz, H_{arom}), 7.90 (t, 1H, J = 7.53 Hz, H_{arom}), 7.61 (t, 1H, J = 7.64 Hz, H_{arom}), 7.30 (dd, 1H, J_1 = 8.18 Hz, J_2 = 4.77 Hz, H_{arom}), 3.96 (t, 2H, J = 6.79 Hz, CH_2), 2.46 (t, 2H, J = 6.37 Hz, CH_2), 2.23 (s, 6H, CH_3), 1.98 – 1.89 (m, 2H, CH_2); ^{13}C NMR (75 MHz, DMSO-d_6): δ/ppm = 157.1, 151.6, 151.1, 145.6, 135.1, 133.6, 125.4, 124.5, 123.8, 121.5, 117.8, 116.9, 116.9, 116.5, 71.4, 57.4, 45.5 (2C), 44.3, 26.6; Found: C, 69.70; H, 5.68; N, 24.62. Calc. for $C_{20}H_{20}N_6$: C, 69.75; H, 5.85; N, 24.40%; MS (ESI) m/z 345.1 $[M+H]^+$.

5-(N-isobutylamino)pyrido[2',3':4,5]imidazo[1,2-a]quinoline-6-carbonitrile ***32***

Compound **32** was prepared using above described method from **22** (0.060 mg, 0.23 mmol) and isobutylamine (0.15 mL, 1.42 mmol) after 4 h of irradiation to yield 0.021 mg (22%) of yellow powder; mp 222–224 °C; ^{1}H NMR (300 MHz, DMSO-d_6): δ/ppm = 8.79 (dd, 1H, J_1 = 8.28 Hz, J_2 = 1.20 Hz, H_{arom}), 8.61 (d, 1H, J = 8.19 Hz, H_{arom}), 8.53 (d, 1H, J = 8.23 Hz, H_{arom}), 8.50 (dd, 1H, J_1 = 4.95 Hz, J_2 = 1.30 Hz, H_{arom}), 8.41 (t, 1H, J = 6.27 Hz, NH_{amin}), 7.92 (t, 1H, J = 7.80 Hz, H_{arom}), 7.62 (t, 1H, J = 7.61 Hz, H_{arom}), 7.30 (dd, 1H, J_1 = 8.19 Hz, J_2 = 4.83 Hz, H_{arom}), 3.70 (t, 2H, J = 6.70 Hz, CH_2), 2.28 – 2.12 (m, 1H, CH), 1.01 (d, 6H, J = 6.60 Hz, CH_3); ^{13}C NMR (75 MHz, DMSO-d_6): δ/ppm = 156.6, 151.1, 150.5, 145.1, 134.7, 133.2, 124.8, 124.5, 123.3, 121.0, 117.2, 116.4, 116.4, 116.1, 71.5, 50.9, 28.2, 19.5; Found: C, 72.45; H, 5.52; N, 22.03. Calc. for $C_{19}H_{17}N_5$: C, 72.36; H, 5.43; N, 22.21%; MS (ESI) m/z 316.1 $[M+H]^+$.

5-(N-piperidin-1-yl)pyrido[2',3':4,5]imidazo[1,2-a]quinoline-6-carbonitrile ***33***

Compound **26** was prepared using above described method from **20** (0.080 mg, 0.29 mmol)

and piperidine (0.21 mL, 2.13 mmol) after 4 h of irradiation to yield 0.030 mg (31%) of yellow powder; mp>300 °C; ^{1}H NMR (600 MHz, DMSO-d_6): δ/ppm = 8.98 (dd, 1H, J_1 = 8.40 Hz, J_2 = 1.38 Hz, H_{arom}), 8.72 (d, 1H, J = 7.98 Hz, H_{arom}), 8.62 (dd, 1H, J_1 = 4.68 Hz, J_2 = 1.32 Hz, H_{arom}), 8.16 (dd, 1H, J_1 = 8.22 Hz, J_2 = 1.38 Hz, H_{arom}), 7.96 (td, 1H, J_1 = 7.77 Hz, J_2 = 1.41 Hz, H_{arom}), 7.66 (td, 1H, J_1 = 7.65 Hz, J_2 = 0.78 Hz, H_{arom}), 7.43 (dd, 1H, J_1 = 8.31 Hz, J_2 = 4.71 Hz, H_{arom}), 3.64 (t, 4H, J = 5.22 Hz, CH_2), 1.87 – 1.82 (m, 4H, CH_2), 1.77 – 1.71 (m, 2H, CH_2); ^{13}C NMR (75 MHz, DMSO-d_6): δ/ppm = not enough soluble; Found: C, 73.49; H, 5.26; N, 21.25. Calc. for $C_{20}H_{17}N_5$: C, 73.37; H, 5.23; N, 21.39%; MS (ESI) m/z 328.1 $[M+H]^+$.

*5-(N-piperazin-1-yl)pyrido[2',3':4,5]imidazo[1,2-a]quinoline-6-carbonitrile **34***

Compound **34** was prepared using above described method from **22** (0.070 mg, 0.20 mmol) and piperazine (0.108 mg, 1.30 mmol) after 4 h of irradiation to yield 0.062 mg (76%) of yellow powder; mp 276–280 °C; ^{1}H NMR (600 MHz, DMSO-d_6): δ/ppm = 8.93 (dd, 1H, J_1 = 8.34 Hz, J_2 = 1.32 Hz, H_{arom}), 8.66 (d, 1H, J = 8.28 Hz, H_{arom}), 8.61 (dd, 1H, J_1 = 4.68 Hz, J_2 = 1.32 Hz, H_{arom}), 8.16 (dd, 1H, J_1 = 8.22 Hz, J_2 = 1.32 Hz, H_{arom}), 7.92 (td, 1H, J_1 = 7.80 Hz, J_2 = 1.35 Hz, H_{arom}), 7.61 (td, 1H, J_1 = 7.53 Hz, J_2 = 0.66 Hz, H_{arom}), 7.41 (dd, 1H, J_1 = 8.25 Hz, J_2 = 4.71 Hz, H_{arom}), 3.58 (t, 4H, J = 4.74 Hz, CH_2), 3.00 (t, 4H, J = 4.74 Hz, CH_2), 2.06 (s, 1H, NH); ^{13}C NMR (75 MHz, DMSO-d_6): δ/ppm = 158.8, 156.4, 149.5, 146.6, 136.3, 133.8, 131.8, 128.4, 125.5, 123.5, 122.6, 119.8, 117.7, 116.9, 116.4, 88.0, 54.5, 46.5; Found: C, 69.62; H, 4.75; N, 25.63. Calc. for $C_{19}H_{16}N_6$: C, 69.50; H, 4.91; N, 25.59%; MS (ESI) m/z 329.1 $[M+H]^+$.

4.2.3. Synthesis of 2,5-diamino substituted pyrido[3',2':4,5]imidazo[1,2-*a*]quinoline-6-carbonitriles and pyrido[2',3':4,5]imidazo[1,2-*a*]quinoline-6-carbonitriles

*(Z)-3-(2-chloro-4-fluorophenyl)-3-hydroxy-2-(3H-imidazo[4,5-b]pyridin-2-yl)acrylonitrile **17***

A solution of 1.000 g (6.32 mmol) 2-(1*H*-imidazo[4,5-*b*]pyridin-2-yl)acetonitrile **2** and 1.220 g (6.32 mmol) 2-chloro-4-fluorobenzoylchloride **15** in pyridine (7 mL) was refluxed for 1.5 h. The cooled mixture was poured into water (50 mL) and the resulting product was filtered off and recrystallized from ethanol to obtain a brown powder (0.950 g, 47%); mp 275–279 °C; ^{1}H NMR (300 MHz, DMSO-d_6): δ/ppm = 13.68 (bs, 1H, OH), 13.24 (bs, 1H, $H_{imidazopyridine}$), 8.28 (dd, 1H, J = 5.10 Hz, H_{arom}), 7.98 (d, 1H, J = 7.77 Hz, H_{arom}), 7.57 – 7.48 (m, 2H, H_{arom}), 7.35 – 7.27 (m, 2H, H_{arom}); ^{13}C NMR (75 MHz, DMSO-d_6): δ/ppm = 185.6, 163.9 (d, J_{CF} = 247.31 Hz), 154.7, 146.5, 140.9, 137.6 (d, J_{CF} = 3.45 Hz), 131.3 (d, J_{CF} = 10.81 Hz), 130.6 (d, J_{CF} =

9.13 Hz), 126.2, 121.4, 120.1, 118.6, 117.4 (d, J_{CF} = 24.94 Hz), 114.9 (d, J_{CF} = 21.12 Hz), 69.9; Found: C, 57.00; H, 2.66; N, 18.01. Calc. for $C_{15}H_8ClFN_4O$: C, 57.25; H, 2.56; N, 17.80%; MS (ESI) m/z 315.0 $[M+H]^+$.

2-fluoro-5-oxo-5,7-dihydropyrido[3',2':4,5]imidazo[1,2-a]quinoline-6-carbonitrile ***19a*** *and 2-fluoro-5-oxo-5,7-dihydropyrido[2',3':4,5]imidazo[1,2-a]quinoline-6-carbonitrile* ***19b***

A solution of 1.280 g (4.07 mmol) (*Z*)-3-(2-chloro-4-fluorophenyl)-3-hydroxy-2-(3H-imidazo[4,5-*b*]pyridin-2-yl)acrylonitrile **17** and 1.130 g *t*-KOBu in DMF (15 mL) was refluxed for 2 h. After cooling, the reaction mixture was evaporated under vacuum and dissolved in water (50 mL). The resulting product was filtered off and recrystallized from ethanol to obtain a light brown powder (0.488 g, 43%) in the form of a mixture of regioisomers in the ratio **19a:19b** = 1:4; **19a**: ^{1}H NMR (300 MHz, DMSO-d_6): δ/ppm = 9,34 (dd, 1H, J_1 = 11,28 Hz, J_2 = 2,61 Hz, H_{arom}), 8,31 – 8,29 (m, 1H, H_{arom}), 8,23 – 8,17 (m, 2H, H_{arom}), 7,78 (dd, 1H, J_1 = 7,86 Hz, J_2 = 1,47 Hz, H_{arom}), 7,28 – 7,26 (m, 1H, H_{arom}); **19b**: ^{1}H NMR (300 MHz, DMSO-d_6): δ/ppm = 8,56 (dd, 1H, J_1 = 8,09 Hz, J_2 = 1,65 Hz, H_{arom}), 8,33 – 8,26 (m, 2H, H_{arom}), 8,15 – 8,10 (m, 1H, H_{arom}), 7,26 (td, 1H, J_1 = 9,42 Hz, J_2 = 2,21 Hz, H_{arom}), 7,06 (dd, 1H, J_1 = 8,00 Hz, J_2 = 4,94 Hz, H_{arom}); MS (ESI) m/z 279.0 $[M+H]^+$.

5-chloro-2-fluoropyrido[3',2':4,5]imidazo[1,2-a]quinoline-6-carbonitrile 21 and 5-chloro-2-fluoropyrido[2',3':4,5]imidazo[1,2-a]quinoline-6-carbonitrile ***23***

A solution of 0.500 g (1.85 mmol) **19a** and **19b**, 0.107 g PCl_5 in $POCl_3$ (11 mL) was refluxed for 1.5 h. After cooling, the reaction mixture was evaporated under vacuum and dissolved in water (10 ml). The resulting product was filtered off and washed with water to obtain a yellow powder (0.217 g, 39%) in the form of a mixture of regioisomers in the ratio **21:23** = 1:4 separated by column chromatography on SiO_2 using CH_2Cl_2/methanol as eluent.

21: 0.038 g; mp 289–290 °C; ^{1}H NMR (300 MHz, DMSO-d_6): δ/ppm = 9.50 (dd, 1H , J_1 = 10.50 Hz, J_2 = 2.49 Hz, H_{arom}), 8.69 (dd, 1H , J_1 = 4.71 Hz, J_2 = 1.38 Hz, H_{arom}), 8.44 (dd, 1H, J_1 = 8.19 Hz, J_2 = 1.41 Hz, H_{arom}), 8.38 (dd, 1H , J_1 = 9.14 Hz, J_2 = 1.41 Hz, H_{arom}), 7.70 (dd, 1H, J_1 = 6.81 Hz, J_2 = 3.30 Hz, H_{arom}), 7.64 (td, 1H, J_1 = 7.91 Hz, J_2 = 2.58 Hz, H_{arom}); ^{13}C NMR (75 MHz, DMSO-d_6): δ/ppm = 167.2, 163.8, 145.2, 144.9, 136.8, 131.0 (d, J_{CF} = 10.95 Hz), 128.96, 122.0, 116.8, 115.2 (d, J_{CF} = 23.52 Hz), 113.3, 104.7 (d, J_{CF} = 28.96 Hz), 86.60; Found: C, 60.56; H, 1.96; N, 19.01. Calc. for $C_{15}H_6ClFN_4$: C, 60.73; H, 2.04; N, 18.88%; MS (ESI) m/z 297.0 $[M+H]^+$.

23: 0.170 g; mp>300 °C; ^{1}H NMR (300 MHz, DMSO-d_6): δ/ppm = 9.29 (dd, 1H, J_1 = 8.49

Hz, J_2 = 1.14 Hz, H_{arom}), 8.81 (dd, 1H, J_1 = 4.67 Hz, J_2 = 1.16 Hz, H_{arom}), 8.70 (dd, 1H, J_1 = 10.13 Hz, J_2 = 2.30 Hz, H_{arom}), 8.52 (dd, 1H, J_1 = 9.14 Hz, J_2 = 6.05 Hz, H_{arom}), 7.73 (td, 1H, J_1 = 8.63 Hz, J_2 = 2.24 Hz, H_{arom}), 7.61 (dd, 1H, J_1 = 8.46 Hz, J_2 = 4.68 Hz, H_{arom}); ^{13}C NMR (75 MHz, DMSO-d_6): δ/ppm = 167.5, 152.5, 148.2, 143.7, 131.9, 131.1, 124.1, 123.6, 119.4, 115.3 (d, J_{CF} = 23.55 Hz), 104.5 (d, J_{CF} = 27.53 Hz); Found: C, 60.81; H, 2.15; N, 18.68. Calc. for $C_{15}H_6ClFN_4$: C, 60.73; H, 2.04; N, 18.88%; MS (ESI) m/z 297.0 $[M+H]^+$.

2,5-bis(N-isobutylamino)pyrido[3',2':4,5]imidazo[1,2-a]quinoline-6-carbonitrile ***28***

Compound **28** was prepared using above described method from **21** (0.060 mg, 0.20 mmol) and isobutylamine (0.15 mL, 1.42 mmol) after 4 h of irradiation to yield 0.027 mg (35%) of yellow oil; ^{1}H NMR (300 MHz, DMSO-d_6): δ/ppm = 8.97 (d, 1H, J = 2.31 Hz, H_{arom}), 8.32 (dd, 1H, J_1 = 4.80 Hz, J_2 = 1.41 Hz, H_{arom}), 8.15 (d, 1H, J = 9.27 Hz, H_{arom}), 8.02 (dd, 1H, J_1 = 7.98 Hz, J_2 = 1.35 Hz, H_{arom}), 7.92 (t, 1H, J = 5.55 Hz, NH_{amin}), 6.40 (dd, 1H, J_1 = 8.01 Hz, J_2 = 4.83 Hz, H_{arom}), 7.17 (t, 1H, J = 5.55 Hz, NH_{amin}), 6.83 (dd, 1H, J_1 = 9.15 Hz, J_2 = 2.28 Hz, H_{arom}), 3.63 (t, 2H, J = 6.66 Hz, CH_2), 3.06 (t, 2H, J = 6.17 Hz, CH_2), 2.20 – 2.09 (m, 1H, CH), 2.05 – 1.93 (m, 1H, CH), 1.01 (d, 6H, J = 6.69 Hz, CH_3), 0.98 (d, 6H, J = 6.63 Hz, CH_3); ^{13}C NMR (150 MHz, DMSO-d_6): δ/ppm = 152.8, 151.5, 150.5, 146.2, 139.9, 137.1, 136.6, 124.9 (2C), 124.4, 119.5 (2C), 118.2, 104.1, 67.6, 50.8, 50.4, 28.3, 27.3, 20.3, 19.5; Found: C, 71.32; H, 6.52; N, 22.14. Calc. for $C_{23}H_{26}N_6$: C, 71.47; H, 6.78; N, 21.74%; MS (ESI) m/z 387.1 $[M+H]^+$.

2,5-di(N-piperidin-1-yl)pyrido[3',2':4,5]imidazo[1,2-a]quinoline-6-carbonitrile ***29***

Compound **29** was prepared using above described method from **21** (0.060 mg, 0.20 mmol) and piperidine (0.21 mL, 2.13 mmol) after 4 h of irradiation to yield 0.030 mg (36%) of orange powder; mp>300 °C; ^{1}H NMR (600 MHz, DMSO-d_6): δ/ppm = 9.30 (d, 1H, J = 1.50 Hz, H_{arom}), 8.49 (d, 1H, J = 4.44 Hz, H_{arom}), 8.19 (d, 1H, J = 8.10 Hz, H_{arom}), 7.86 (d, 1H, J = 9.84 Hz, H_{arom}), 7.51 (dd, 1H, J_1 = 7.98 Hz, J_2 = 4.80 Hz, H_{arom}), 7.23 (dd, 1H, J_1 = 9.39 Hz, J_2 = 1.95 Hz, H_{arom}), 3.58 (bs, 8H, CH_2), 1.81 (bs, 4H, CH_2), 1.73 (bs, 2H, CH_2), 1.68 (bs, 6H, CH_2); ^{13}C NMR (75 MHz, DMSO-d_6): δ/ppm = 153.9, 141.9, 138.2, 137.3, 135.4, 128.8, 126.3, 120.6, 117.0, 112.3, 99.8, 54.2 (2C), 48.3 (2C), 26.7 (2C), 25.4 (2C), 24.3, 24.2; Found: C, 73.00; H, 6.28; N, 20.72. Calc. for $C_{25}H_{26}N_6$: C, 73.14; H, 6.38; N, 20.47%; MS (ESI) m/z 411.2 $[M+H]^+$.

2,5-(N-piperazin-1-yl)pyrido[3',2':4,5]imidazo[1,2-a]quinoline-6-carbonitrile ***30***

Compound **30** was prepared using above described method from **21** (0.055 mg, 0.19 mmol)

and piperazine (0.080 mg, 0.93 mmol) after 4 h of irradiation to yield 0.074 mg (97%) of yellow powder; mp > 300 °C; ^{1}H NMR (400 MHz, DMSO-d_6): δ/ppm = 9.28 (d, 1H, J = 2.48 Hz, H_{arom}), 8.50 (dd, 1H, J_1 = 4.78 Hz, J_2 = 1.50 Hz, H_{arom}), 8.22 (dd, 1H, J_1 = 8.14 Hz, J_2 = 1.50 Hz, H_{arom}), 7.92 (d, 1H, J = 9.56 Hz, H_{arom}), 7.52 (dd, 1H, J_1 = 8.10 Hz, J_2 = 4.82 Hz, H_{arom}), 7.24 (dd, 1H, J_1 = 9.24 Hz, J_2 = 2.60 Hz, H_{arom}), 3.64 (t, 4H, J = 4.56 Hz, CH_2), 3.55 (t, 4H, J = 4.88 Hz, CH_2), 3.15 (t, 4H, J = 4.38 Hz, CH_2), 3.06 (t, 4H, J = 5.06 Hz, CH_2); ^{13}C NMR (100 MHz, DMSO-d_6): δ/ppm = 168.9, 159.0, 153.8, 142.4, 138.1, 137.3, 128.9, 126.8, 120.8, 112.6, 109.9, 100.2, 52.5, 46.7, 45.4, 44.7; Found: C, 66.82; H, 5.79; N, 27.39. Calc. for $C_{23}H_{24}N_8$: C, 66.97; H, 5.86; N, 27.17%; MS (ESI) m/z 413.1 $[M+H]^+$.

2,5-bis(N-isobutylamino)pyrido[2',3':4,5]imidazo[1,2-a]quinoline-6-carbonitrile ***35***

Compound **35** was prepared using above described method from **22** (0.060 mg, 0.20 mmol) and isobutylamine (0.15 mL, 1.42 mmol) after 4 h of irradiation to yield 0.035 mg (45%) of yellow powder; mp 289–292 °C; ^{1}H NMR (600 MHz, DMSO-d_6): δ/ppm = 8.57 (d, 1H, J = 8.10 Hz, H_{arom}), 8.46 (d, 1H, J = 4.68 Hz, H_{arom}), 8.21 (d, 1H, J = 9.24 Hz, H_{arom}), 7.96 (t, 1H, J = 5.40 Hz, NH_{amin}), 7.55 (bs, 1H, H_{arom}), 7.28 (dd, 1H, J_1 = 8.07 Hz, J_2 = 4.83 Hz, H_{arom}), 7.02 (t, 1H, J = 5.40 Hz, NH_{amin}), 6.84 (dd, 1H, J_1 = 9.12 Hz, J_2 = 1.32 Hz, H_{arom}), 3.64 (t, 2H, J = 6.69 Hz, CH_2), 3.10 (t, 2H, J = 6.09 Hz, CH_2), 2.17 – 2.12 (m, 1H, CH), 1.96 – 1.90 (m, 1H, CH), 1.02 (d, 6H, J = 6.60 Hz, CH_3), 0.98 (d, 6H, J = 6.60 Hz, CH_3); ^{13}C NMR (150 MHz, DMSO-d_6): δ/ppm = 157.0, 153.1, 152.3, 151.2, 144.7, 136.6, 126.1, 123.2, 120.3 (2C), 118.1, 115.3 (2C), 104.4, 68.1, 50.8, 50.0, 28.3, 27.7, 20.3, 19.5, Found: C, 71.52; H, 6.92; N, 21.56. Calc. for $C_{23}H_{26}N_6$: C, 71.47; H, 6.78; N, 21.74%; MS (ESI) m/z 387.2 $[M+H]^+$.

2,5-di(N-piperidin-1-yl)pyrido[2',3':4,5]imidazo[1,2-a]quinoline-6-carbonitrile ***36***

Compound **36** was prepared using above described method from **22** (0.060 mg, 0.20 mmol) yellow powder; mp>300 °C; ^{1}H NMR (600 MHz, DMSO-d_6): δ/ppm = 8.69 (d, 1H, J = 8.28 Hz, H_{arom}), 8.59 (dd, 1H, J_1 = 4.71 Hz, J_2 = 1.23 Hz, H_{arom}), 7.89 (d, 1H, J = 9.36 Hz, H_{arom}), 7.55 (d, 1H, J = 2.04 Hz, H_{arom}), 7.38 (dd, 1H, J_1 = 8.22 Hz, J_2 = 4.74 Hz, H_{arom}), 7.24 (dd, 1H, J_1 = 9.42 Hz, J_2 = 2.22 Hz, H_{arom}), 3.60 (bs, 8H, CH_2), 1.81 (bs, 4H, CH_2), 1.74 (bs, 2H, CH_2), 1.69 (bs, 6H, CH_2); ^{13}C NMR (150 MHz, DMSO-d_6): δ/ppm = 158.9, 156.3, 153.4, 150.4, 145.6, 138.2, 129.0, 122.8, 121.8, 116.7, 116.6, 111.9, 108.8, 97.3, 82.7, 53.7 (2C), 47.8 (2C), 26.1 (2C), 24.9 (2C), 23.7, 23.6; Found: C, 73.34; H, 6.30; N, 20.36. Calc. for $C_{25}H_{26}N_6$: C, 73.14; H, 6.38; N, 20.47%; MS (ESI) m/z 411.1 $[M+H]^+$.

2,5-(N-piperazin-1-yl)pyrido[2',3':4,5]imidazo[1,2-a]quinoline-6-carbonitrile ***37***

Compound **37** was prepared using above described method from **23** (0.060 mg, 0.20 mmol)

and piperazine (0.090 mg, 1.01 mmol) after 4 h of irradiation to yield 0.062 mg (75%) of yellow powder; mp > 300 °C; ^{1}H NMR (400 MHz, DMSO-d_6): δ/ppm = 8.76 (d, 1H, J = 8.96 Hz, H_{arom}), 8.60 (d, 1H, J = 5.00 Hz, H_{arom}), 7.95 (d, 1H, J = 9.28 Hz, H_{arom}), 7.59 (d, 1H, J = 4.48 Hz, H_{arom}), 7.39 (dd, 1H, J_1 = 8.04 Hz, J_2 = 5.32 Hz, H_{arom}), 7.25 (d, 1H, J = 9.64 Hz, H_{arom}), 3.60 (t, 4H, J = 4.24 Hz, CH_2), 3.56 (t, 4H, J = 3.94 Hz, CH_2), 3.07 (t, 4H, J = 4.02 Hz, CH_2), 2.99 (t, 4H, J = 4.78 Hz, CH_2); ^{13}C NMR (100 MHz, DMSO-d_6): δ/ppm = not enough soluble; Found: C, 67.09; H, 5.98; N, 26.93. Calc. for $C_{23}H_{24}N_8$: C, 66.97; H, 5.86; N, 27.17%; MS (ESI) m/z 413.1 $[M+H]^+$.

3.3. Antiproliferative activity *in vitro*

The experiments were carried out on three human cell lines: HCT 116 (colon carcinoma), H 460 (lung carcinoma), MCF-7 (breast carcinoma) and HEK 293 (human embryonic kidney cells), according to the previously published experimental procedure. Briefly, the cells were grown in DMEM medium with the addition of 10% fetal bovine serum (FBS), 2 mM L-glutamine, 100 U/mL penicillin and 100 μg/mL streptomycin, and cultured as monolayers at 37 °C in a humidified atmosphere with 5% CO_2. Cells were seeded at 2×10^3 cells/well in standard 96-well microtiter plates and left to attach for 24 h. The next day, the test compound was added in five serial 10-fold dilutions. The cell growth rate was evaluated after 72 h of incubation, using MTT assay. Obtained results are expressed as IC_{50} value which stands for the concentration of the compound necessary for 50% of growth inhibition. The IC_{50} values are calculated from the concentration-response curve using linear regression analysis by fitting the test concentrations that give PG values above and below the reference value (i.e. 50%). Each test was performed in quadruplicate in at least two individual experiments.

3.4. DNA/RNA binding study

The UV/vis spectra were recorded on a Varian Cary 100 Bio spectrophotometer, CD spectra on JASCO J815 spectrophotometer and fluorescence spectra on a Varian Cary Eclipse spectrophotometer at 25ºC using appropriate 1cm path quartz cuvettes.

Materials. Polynucleotides were purchased as noted: poly A–poly U, calf thymus ctDNA, poly(dAdT)$_2$ and poly(dGdC)$_2$ (Sigma-Aldrich). Polynucleotides were dissolved in Na-cacodylate buffer, I=0.05 mol dm^{-3}, pH=7. The calf thymus ctDNA was additionally sonicated and filtered through a 0.45 mm filter.[54] Polynucleotide concentration was determined spectroscopically as the concentration of phosphates.[55]

Spectrophotometric titrations were performed at pH=7 (I=0.05 mol dm^{-3}, sodium cacodylate buffer) by adding portions of polynucleotide solution into the solution of the studied compound for fluorimetric experiments and CD experiments were done by adding portions of the compound stock solution into the solution of a polynucleotide. In fluorimetric experiments excitation wavelength of λ_{exc}=364/365,397,408 and 428/429 nm was used to avoid the inner filter effect caused due to increasing absorbance of the polynucleotide. Emission was collected in the range λ_{em}=400–650 nm. Values for K_s obtained by processing titration data using the Scatchard equation (Table 2), all have satisfactory correlation coefficients (≥0.99). Thermal melting curves for DNA, RNA and their complexes with studied compounds were determined as previously described by following the absorption change at 260 nm as a function of temperature. The absorbance of the ligands was subtracted from every curve and the absorbance scale was normalized. T_m values are the midpoints of the transition curves determined from the maximum of the first derivative and checked graphically by the tangent method. The ΔT_m values were calculated by subtracting T_m of the free nucleic acid from T_m of the complex. Every ΔT_m value here reported was the average of two measurements. The error in ΔT_m is ±0.5ºC. 5'- AGGG(TTAGGG)$_3$–3'(Tel22) was obtained from IDT (Integrated DNA Technologies), USA. Tel22 was dissolved in 0.1 M potassium phosphate buffer. The starting Tel22 oligonucleotide solution was first heated up to 95ºC for 10 min and then slowly cooled to 10ºC at the cooling rate of 1ºC/ min to allow DNA oligonucleotide to adopt a G-quadruplex structure.[56] The G-quadruplex structure was confirmed by thermal melting and CD spectra.[41] The concentration of G quadruplex was expressed in terms of oligonucleotide structure. In fluorimetric titrations, aliquots of Tel 22 solution were added to the solution of ligands (c = 5 x 10^{-7} M).

4. Acknowledgments

We greatly appreciate the financial support of the Croatian Science Foundation under the projects IP-2018-01-4379 entitled *Exploring the antioxidative potential of benzazole scaffold in the design of novel antitumor agents* and IP-2018-01-4694 entitled *Molecular recognition of DNA:RNA hybrid and multistranded structures in bioanalytical and in vitro systems*.

6. Conflict of interests

The authors declare no conflict of interest.

References

1. J. Joule, K. Mills, *Heterocyclic chemistry*, 5th Edition, Blackwell Publishing Ltd, **2010**.

2. A. C. Foster, J. A.Kemp, Glutamate- and GABA-based CNS therapeutics, Curr. Opin. Pharmacol. 6 (2006) 7–17. Doi: 10.1016/j.coph.2005.11.005.

3. M. Dowsett, D. Smithers, J. Moore, P. F. Trunet, R. C. Coombes, T. J. Powles, R. Rubens, I. E. Smith, Endocrine changes with the aromatase inhibitor fadrozole hydrochloride in breast cancer, Eur. J. Cancer 30 (1994) 1453–1458. Doi:10.1016/0959-8049(94)00281-9

4. N. Ando, S. Terashima, Synthesis and matrix metalloproteinase (MMP)-12 inhibitory activity of ageladine A and its analogs, Bioorg. Med. Chem. Lett. 17 (2007) 4495–4499. Doi: 10.1016/j.bmcl.2007.06.005

5. M. Hranjec, B. Lučić, I. Ratkaj, S. K. Pavelić, I. Piantanida, K. Pavelić, G. Karminski-Zamola, Novel imidazo[4,5-*b*]pyridine and triaza-benzo[*c*]fluorene derivatives: Synthesis, antiproliferative activity and DNA binding studies, Eur. J. Med. Chem. 46 (2011) 2748–2758. Doi: 10.1016/j.ejmech.2011.03.062

6. M. Bamford, 3 H+/K+ ATPase inhibitors in the treatment of acid-related disorders, Prog. Med. Chem. 47 (2009) 75–162. Doi: 10.1016/S0079-6468(08)00203-8.

7. P. Lan, W. N. Chen, W. M. Chen, Molecular modeling studies on imidazo[4,5-*b*]pyridine derivatives as Aurora A kinase inhibitors using 3D-QSAR and docking approaches, Eur. J. Med. Chem. 46 (2011) 77-94. Doi: j.ejmech.2010.10.017.

8. V. Bavetsias, J. M. Large, C. Sun, N. Bouloc, M. Kosmopoulou, M. Matteucci, N. E. Wilsher, V. Martins, J. Reynisson, B. Atrash, A. Faisal, F. Urban, M. Valenti, A. de Haven Brandon, G. Box, F. I. Raynaud, P. Workman, S. A. Eccles, R. Bayliss, J. Blagg, S. Linardopoulos, E. McDonald, Imidazo[4,5-*b*]pyridine derivatives as inhibitors of Aurora kinases: lead optimization studies toward the identification of an orally bioavailable preclinical development candidate, J. Med. Chem.53 (14) (2010) 5213-5228. Doi: 10.1021/jm100262j.

9. B. J. Newhouse, S. Wenglowsky, J. Grina, E. R. Laird, W. C. Voegtli, L. Ren, K. Ahrendt, A. Buckmelter, S. L. Gloor, N. Klopfenstein, et al, Imidazo[4,5-*b*]pyridine inhibitors of B-Raf kinase, Bioor . Med. Chem. Lett. 23 (2013) 5896–5899. Doi:10.1016/j.bmcl.2013.08.086

10. C. Scarpignato, R. H. Hunt, Proton pump inhibitors: The beginning of the end or the end of the beginning?, Curr. Opin. Pharmacol. 8 (2008) 677–684. Doi:10.1016/j.coph.2008.09.004

11. V. Bavetsias, C. Sun, N. Bouloc, J. Reynisson, P. Workman, S. Linardopoulos, E. McDonald, Hit generation and exploration: Imidazo[4,5-*b*]pyridine derivatives as inhibitors

of Aurora kinases, Bioorg. Med. Chem. Lett. 17 (2007) 6567–6571. Doi:10.1016/j.bmcl.2007.09.076.

12. V. Bavetsias, Y. Pérez-Fuertes, P. J. McIntyre, B. Atrash, M. Kosmopoulou, L. O'Fee, R. Burke, C. Sun, A. Faisal, K. Bush, S. Avery, A. Henley, F. I. Raynaud, S. Linardopoulos, R. Bayliss, J. Blagg, 7-(Pyrazol-4-yl)-3H-imidazo[4,5-*b*]pyridine-based derivatives for kinase inhibition: Co-crystallisation studies with Aurora-A reveal distinct differences in the orientation of the pyrazole N1-substituent, Bioorg. Med. Chem. Lett. 25 (2015) 4203–4209. Doi:10.1016/j.bmcl.2015.08.003

13. M. M. Vasbinder, M. Alimzhanov, M. Augustin, G. Bebernitz, K. Bell, C. Chuaqui, T. Deegan, A. D. Ferguson, K. Goodwin, D. Huszar, et al, Identification of azabenzimidazoles as potent JAK1 selective inhibitors, Bioorg. Med. Chem. Lett. 26 (2016) 60–67. Doi:10.1016/j.bmcl.2015.11.031

14. B. J. Newhouse, S. Wenglowsky, J. Grina, E. R. Laird, W. C. Voegtli, L. Ren, K. Ahrendt, A. Buckmelter, S. L. Gloor, N. Klopfenstein, J. Rudolph, Z. Wen, X. Li, B. Feng, Imidazo[4,5-*b*]pyridine inhibitors of B-Raf kinase, Bioorg. Med. Chem. Lett. 23 (2013) 5896-5899. Doi:10.1016/j.bmcl.2013.08.086.

15. T. Baladi, J. Aziz, F. Dufour, V. Abet, V. Stoven, F. Radvanyi, F. Poyer, T.-D. Wu, J.-L. Guerquin-Kern, I. Bernard-Pierrot, S. Marco Garrido, S. Piguel, Bioorg. Med. Chem. 26 (2018) 5510-5530. Doi:10.1016/j.bmc.2018.09.031.

16. N. M. Ghanema, F. Farouka, R. F. Georgeb, S. E. S. Abbasb, O. M. El-Badrya, Design and synthesis of novel imidazo[4,5-*b*]pyridine based compounds as potent anticancer agents with CDK9 inhibitory activity, Bioorg. Chem. 80 (2018) 565–576. Doi: 10.1016/j.bioorg.2018.07.006.

17. X. D. An, H. Liu, Z. L. Xu, Y. Jin, X. Peng, Y. M. Yao, M. Geng, Y. Q. Long, et al, Discovery of potent 1H-imidazo[4,5-*b*]pyridine-based c-Met kinase inhibitors via mechanism-directed structural optimization, Bioorg. Med. Chem. Lett. 25 (2015) 708–716. Doi:10.1016/j.bmcl.2014.11.070

18. A. M. Sajith, K. K. A. Khader, N. Joshi, M. N. Reddy, M. Syed Ali Padusha, H. P. Nagaswarupa, M. Nibin Joy, Y. D. Bodke, R. P. Karuvalam, R. Banerjee, A. Muralidharan, P. Rajendra, Design, Synthesis and Structure-Activity Relationship (SAR) studies of Imidazo[4,5-*b*]pyridine derived Purine Isosteres and their Potential as Cytotoxic agents, Eur. J. Med. Chem. 89 (2015) 21-31. Doi:10.1016/j.ejmech.2014.10.037.

19. N. Perin, R. Nhili, K. Ester, W. Laine, G. Karminski-Zamola, M. Kralj, M.-H. David-Cordonnier, M. Hranjec, Synthesis, antiproliferative activity and DNA binding properties of novel 5-Aminobenzimidazo[1,2-*a*]quinoline-6-carbonitriles, Eur. J. Med. Chem. 80 (2014) 218–227. Doi:10.1016/j.ejmech.2014.04.049

20. N. Perin, I. Martin-Kleiner, R. Nhili, W. Laine, M.H. David-Cordonnier, O. Vugrek, G. Karminski-Zamola, M. Kralj, M. Hranjec, Biological activity and DNA binding studies of 2-substituted benzimidazo[1,2-*a*]quinolines bearing different amino side chains, Med. Chem. Comm. 4 (2013) 1537–1550. Doi:10.1039/C3MD00193H

21. M. Demeunynck, C. Bailly, W. D. Wilson, DNA and RNA binders: from small molecules to drugs, Vol.1. Wiley-VCH: Weinheim, (Chapter 5), 2002.

22. N. Perin, R. Nhili, M. Cindrić, B. Bertoša, D. Vušak, I. Martin-Kleiner, W. Laine, G. Karminski-Zamola, M. Kralj, M.-H. David-Cordonnier, M. Hranjec, Amino substituted benzimidazo[1, 2- a]quinolines: Antiproliferative potency, 3D QSAR study and DNA binding properties, Eur. J. Med. Chem. 122 (2016) 530-545. Doi:10.1016/j.ejmech.2016.07.007.

23. J. T. Starr, R. J. Sciotti, D. L. Hanna, M. D. Huband, L. M. Mullins, H. Cai, J. W. Gage, M. Lockard, M. R. Rauckhorst, R. M. Owen, M. S. Lall, M. Tomilo, H. Chen, S. P. McCurdy, M. R. Barbachyn, 5-(2-Pyrimidinyl)-imidazo[1,2-a]pyridines are antibacterial agents targeting the ATPase domains of DNA gyrase and topoisomerase IV, Bioorg. Med. Chem. Lett. 19 (2009) 5302-5306. Doi: 10.1016/j.bmcl.2009.07.141.

24. A. Kamal, G. Ramakrishna, M. Janaki Ramaiah, A. Viswanath, A. V. Subba Rao, C. Bagul, D. Mukhopadyay, S. N. C. V. L. Pushpavalli, M. Pal-Bhadra, Design, synthesis and biological evaluation of imidazo[1,5-a]pyridine–PBD conjugates as potential DNA-directed alkylating agents, Med. Chem. Commun. 4 (2013), 697-703.Doi:https://doi.org/10.1039/C2MD20219K

25. Chemicalize was used for pKa value prediction, (accessed December, 2020), https://chemicalize.com/ developed by ChemAxon (http://www.chemaxon.com).

24. W. Saenger, Principles of nucleic acid structure, Springer-Verlag New York, New York, 1984.

26. J. Olmsted, D. R. Kearns, Mechanism of Ethidium-Bromide Fluorescence Enhancement on Binding to Nucleic-Acids, Biochemistry-Us 16 (1977) 3647–3654. Doi:10.1021/bi00635a022

27. N. W. Luedtke, Q. Liu, Y. Tor, On the electronic structure of ethidium, Chem. Eur. J. 11 (2) (2005) 495–508. Doi:10.1002/chem.200400559

28. H. Szatylowicz, O. Stasyuk, T. M. Krygowski, Substituent Effects in Heterocyclic Systems, In E. F. V. Scriven and C. A. Ramsden, editors: Advances in Heterocyclic Chemistry, pp 137–192. Elsevier Inc. 2015.
29. M. Radić Stojković, I. Piantanida, Tuning urea–phenanthridinium conjugates for DNA/RNA and base pair Recognition, Tetrahedron 64 (2008) 7807-7814. Doi:10.1016/j.tet.2008.05.142
30. I. Piantanida, B. S. Palm, M. Žinić, H. J. Schneider, A new 4,9-diazapyrenium intercalator for single- and double-stranded nucleic acids: distinct differences from related diazapyrenium compounds and ethidium bromide. J. Chem. Soc., Perkin Trans. 2 (2001) 1808-1816. Doi:10.1039/b103214n
31. S. Georghiou, Interaction of acridine drugs with dna and nucleotides, Photochem. Photobiol. 26 (1977) 59-68. Doi:10.1111/j.1751-1097.1977.tb07450.x.
32. S. O. Kelley, J. K. Barton, Electron transfer between bases in double helical DNA, Science, 283 (1999) 375-381. Doi:10.1126/science.283.5400.375.
33. G. Scatchard, The attractions of proteins for small molecules and ions, Ann. N. Y. Acad. Sci. 51 (4) (1949) 660–672. Doi:10.1111/j.1749-6632.1949.tb27297.x
34. J. D. Mcghee, P. H. von Hippel, Correction, J. Mol. Biol. 103 (3) (1976) 679-679. Doi:10.1016/0022-2836(76)90228-X
35. J. L. Mergny, L. Lacroix, Analysis of thermal melting curves, Oligonucleotides 13 (6) (2003) 515–537. Doi:10.1089/154545703322860825
36. N. Berova, K. Nakanishi, R. W. Woody, Circular dichroism Principles and Applications, 2nd Edition, Wiley-VCH, New York, 2000.
37. M. Eriksson, B. Norden, Linear and circular dichroism of drug-nucleic acid complexes, Method Enzymol. 340 (2001) 68–98. Doi:10.1016/S0076-6879(01)40418-6
38. T. Šmidlehner, I. Piantanida, G. Pescitelli, Polarization spectroscopy methods in the determination of interactions of small molecules with nucleic acids - tutorial, Beilstein J. Org. Chem. 14 (2018) 84–105. Doi:10.3762/bjoc.14.5.
39. S. L. Cree, M. A. Kennedy, Relevance of G-quadruplex structures to pharmacogenetics, Front. Pharmacol. 5 (2014) 160. Doi:10.3389/fphar.2014.00160.
40. J. Wang, W. Wang, P. A. Kollman, D. A. Case, Automatic atom type and bond type perception in molecular mechanical calculations, J. Mol. Graph. Model. 25(2) (2006) 247-260. Doi: https://doi.org/10.1016/j.jmgm.2005.12.005.
41. D. A. Case, R. M. Betz, D. S. Cerutti, et al. AMBER16. San Francisco, CA, University of California, 2016.

42. M. Zgarbová, J. Šponer, M. Otyepka, T. E. Cheatham, R. Galindo-Murillo, P. Jurečka, Refinement of the Sugar-Phosphate Backbone Torsion Beta for the AMBER Force Fields Improves the Description of Z-DNA and B-DNA, J. Chem. Theory Comput. 11 (12) (2015) 5723-5736. Doi: https://doi.org/10.1021/acs.jctc.5b00716.

43. J. Wang, R. M. Wolf, J. Caldwell, P. A. Kollman, D. A. Case, Development and testing of a general amber force field, J. Comput. Chem. 25(9) (2004) 1157-1174. Doi: 10.1002/jcc.20035.

44. B. R. Miller, T. D. McGee, J. Swails, N. Homeyer, H. Gohlke, A. Roitberg, MMPBSA.py: an efficient program for end-state free energy calculations, J. Chem. Theory Comput. 8 (2012) 3314-3321. Doi: https://doi.org/10. 1021/ct300418h.

45. J. B. Chaires, Human telomeric G-quadruplex: thermodynamic and kinetic studies of telomeric quadruplex stability, FEBS J. 277 (5) (2010) 1098–1106. Doi:10.1111/j.1742-4658.2009.07462.x.

46. A. T. Phan, V. Kuryavyi, K. N. Luu, D. J. Patel, Structure of two intramolecular G-quadruplexes formed by natural human telomere sequences in K+ solution, Nucleic acids research 35(19) (2007) 6517–6525. Doi:10.1093/nar/gkm706

47. A. Ambrus, D. Chen, J. Dai, T. Bialis, R. A. Jones, D. Yang, Human telomeric sequence forms a hybridtype intramolecular G-quadruplex structure with mixed parallel /antiparallel strands in potassium solution. Nucleic Acids Res, 19, 34(9) (2006) 2723-35. Doi:10.1093/nar/gkl348

48. Y. Xu, Y. Noguchi, H. Sugiyama, The new models of the human telomere d[AGGG(TTAGGG)3] in K+ solution, Bioorg. Med. Chem. 14 (2006) 5584-5591. Doi:10.1016/j.bmc.2006.04.033

49. H. Gampp, M. Maeder, C. J. Meyer, A. D. Zuberbuhler, Calculation of equilibrium constants from multiwavelength spectroscopic data--II: SPECFIT: two user-friendly programs in basic and standard FORTRAN 77, Talanta 32 (4) (1985) 257-64. Doi:10.1016/0039-9140(85)80077-1

50. R. del Villar-Guerra, R. D. Gray, J. B. Chaires, Characterization of quadruplex DNA structure by circular dichroism, Curr. Protoc. Nucleic Acid Chem. 68 (2017) 17.8.1-17.8.16. Doi:10.1002/cpnc.23

51. G. Zagotto, A. Ricci, E. Vasquez, A. Sandoli, S. Benedetti, M. Palumbo, C. Sissi, Tuning G-Quadruplex vs Double-Stranded DNA Recognition in Regioisomeric Lysyl-Peptidyl-Anthraquinone Conjugates, Bioconjugate Chem. 22 (10) (2011) 2126–2135. Doi:10.1021/bc200389w

52. C. I. V. Ramos, S. P. Almeida, L. M. O. Lourenco, P. M. R. Pereira, R. Fernandes, M. A. F. Faustino, J. P. C. Tome, J. Carvalho, C. Cruz, Neves, M. Multicharged Phthalocyanines as Selective Ligands for G-Quadruplex DNA Structures, Molecules 24 (4) (2019) 733. Doi:10.3390/molecules24040733.

53. N. H. Campbell, G. N. Parkinson, A. P. Reszka, S. Neidle, Structural basis of DNA quadruplex recognition by an acridine drug, J. Am. Chem. Soc. 28, 130 (21) (2008) 6722-6724. Doi:10.1021/ja8016973

54. J. B. Chaires, N. Dattagupta, D. M. Crothers, Studies on Interaction of Anthracycline Antibiotics and Deoxyribonucleic-Acid - Equilibrium Binding-Studies on Interaction of Daunomycin with Deoxyribonucleic-Acid, Biochemistry-Us 21 (17) (1982) 3933–3940. Doi:10.1021/bi00260a005

55. T. V. Chalikian, J. Volker, G. E. Plum, K. J. A Breslauer, A more unified picture for the thermodynamics of nucleic acid duplex melting: A characterization by calorimetric and volumetric techniques, P. Natl. Acad. Sci. USA 96 (14) (1999) 7853–7858. Doi:10.1073/pnas.96.14.7853

56. M. Bončina, C. Podlipnik, I. Piantanida, J. Eilmes, M. P. Teulade-Fichou, G. Vesnaver, J. Lah, Thermodynamic fingerprints of ligand binding to human telomeric G-quadruplexes, Nucleic Acids Res. 43 (21) (2015) 10376–10386. Doi:10.1093/nar/gkv1167